

# Mechanics of Sediment Suspension in Well Mixed Estuaries

Adel Mostafa Kamel

Coastal Engineering Limited  
P.O. Box 27  
Dumyat, Egypt 34511

## ABSTRACT

KAMEL, A. M., 1997. Mechanics of sediment suspension in well mixed estuaries. *Journal of Coastal Research*, 14(1), 106-131. Royal Palm Beach (Florida), ISSN 0749-0208.

The equations of conservation of volume, mass, and momentum, and the equation of kinetic energy of turbulence are formulated for the three dimensional flow of a mixture of water and sediment. Their solution gives the profiles of the concentration of suspended sediment, the coefficient of exchange of mass, the turbulent shear stress, and the longitudinal velocity of the flow.

**ADDITIONAL INDEX WORDS:** *Estuaries, Navier-Stokes equations, sedimentation, two component flow, turbulence.*



## SUMMARY

The equations of conservation of volume, of mass, and of momentum, and the equation of kinetic energy of turbulence are formulated for the three dimensional flow of a mixture of water and sediment. The equations are closed and expressed in dimensionless form to represent conditions in well mixed estuaries for ebb flow departing from slack. The method of perturbation is used to reduce the number of terms in each equation by keeping only terms which have large magnitude.

Solution of the zeroth approximation gives the profiles of the concentration of suspended sediment, the coefficient of exchange of mass, the turbulent shear stress, and the longitudinal velocity of the flow. It is found that: (i) the concentration of suspended sediment increases along the estuary, (ii) the coefficient of exchange of mass increases from zero at the bottom to a maximum value at a relative depth of about 0.1 then decreases to a nearly constant value towards the water surface, (iii) the turbulent shear stress increases from zero at the bottom to a maximum value at a relative depth of about 0.2 then decreases towards the water surface, (iv) the turbulent shear stress increases from the center line of the estuary towards the sides of the estuary, and (v) the profile of the longitudinal velocity is nearly logarithmic.

The effect of the concentration of suspended sediment on the turbulent shear stress, the longitudinal velocity of the flow, and von Karman's  $\kappa$  is studied. It is found that an increase in the concentration of suspended sediment would result in: (i) no appreciable change in the profile of the turbulent shear stress, (ii) an increase in the longitudinal velocity of the flow, and (iii) a slight decrease in von Karman's  $\kappa$ . Good agreement is obtained between the analytical findings of this study and the experimental and field data available in the literature.

## INTRODUCTION

The mechanics of sediment suspension has been investigated experimentally for more than five decades and perhaps has reached the stage of a diminishing return. Yet, the question regarding the interdependence between the concentration of suspended sediment and the flow parameters such as the velocity profile, the coefficient of exchange of mass, and the turbulent shear stress remains without a satisfactory answer. An analytical investigation of the subject would be useful in motivating and guiding future experimental research on suspended sediment. To this end this study was undertaken. Estuaries are selected for the study in view of the important functions assigned to estuaries in the human environment. Sediment suspension is studied rather than bed load movement, because the most important shoaling problems arise from the material ordinarily carried in suspension in fresh water streams rather than from the bed load. Well mixed estuaries are investigated rather than salinity stratified estuaries which have added complexities caused by the presence of the fresh-salt water interface.

The problem could be formulated as a two component flow which consists of a mixture of water and sediment or by the principle of continuum mechanics where water and sediment are considered as a continuum with heterogeneous density. A two component flow formulation is adopted herein. SOO (1967) and VASELIEV (1969) reported on two component flow formulations for the equations governing sedimentation. KAMEL (1976) presented a two dimensional formulation for the equations of conservation of volume, of mass, and of momentum and for the equation of kinetic energy of turbulence for a two component flow, water and sediment. The equations were closed, using the semi-empirical theories of turbulence, and were made dimensionless to represent conditions in well mixed estuaries for flow near slack. The method of perturbation was used to reduce the number of terms in each equation by keeping only terms which have large magnitude. Fig-

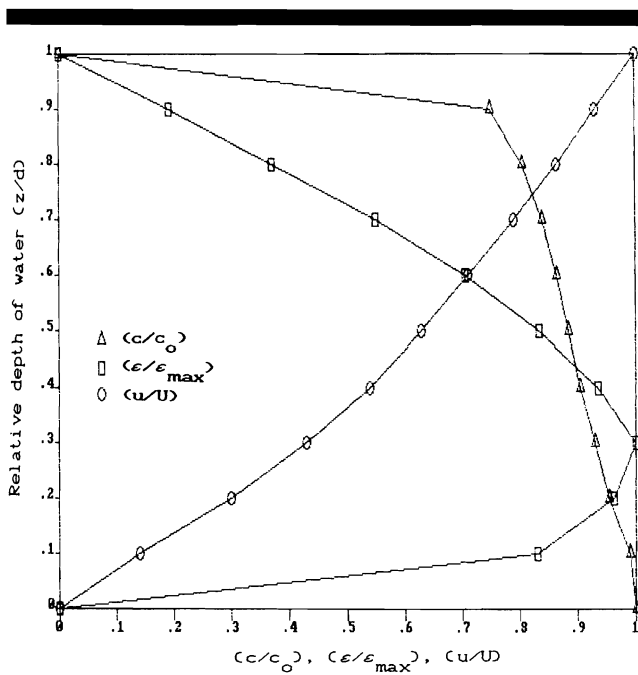


Figure 1. Profiles of the relative concentration of suspended sediment, the relative coefficient of exchange of mass, and the relative longitudinal velocity; the zeroth approximation (Kamel, 1976).

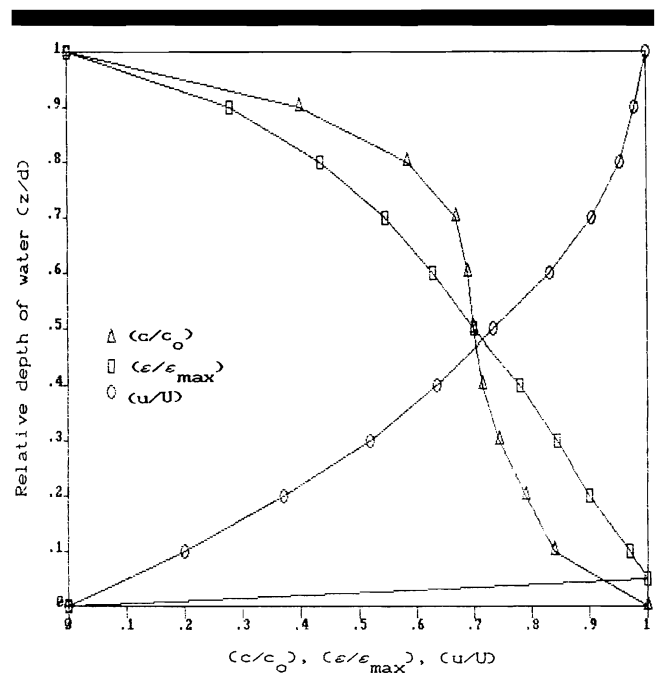


Figure 2. Profiles of the relative concentration of suspended sediment, the relative coefficient of exchange of mass, and the relative longitudinal velocity; the first approximation (Kamel, 1976).

ures 1 and 2 show the results obtained from the solution of the zeroth and the first approximations respectively, for the concentration of suspended sediment, the coefficient of exchange of mass, and the longitudinal velocity. It can be seen from the figures that the profile of the coefficient of exchange of mass obtained from the first approximation has its maximum value closer to the bottom than that obtained from the solution of the zeroth approximation. The figures also show that the velocity profile obtained from the first approximation is closer to a logarithmic velocity profile than that obtained from the zeroth approximation.

In a subsequent study, KAMEL (1978) used quadratures to reduce the equations of the zeroth approximation to a quasi-linear total differential equation in one dependent variable, namely the longitudinal velocity of the flow. Figure 3 shows the three types of velocity profiles obtained from the solution. In Figure 3, profile I is approximately a logarithmic velocity profile, profile II represents return flow near the bottom of the estuary, and profile III represents a density current. In profile III, the non zero velocity at the water surface is due to imposing the boundary condition  $(u/U) = 1$  at the free surface. The equations of the first order perturbation for Rossby number were formulated as integral equations with degenerate kernel which were solved by reducing them to a system of linear algebraic equations. It was proved that the solution of the integral equations exists and is unique. Figure 4 shows profiles of concentration of suspended sediment obtained from the solution of the zeroth approximation and the first order perturbation for Rossby number. It can be seen from the figure that the difference between the two solutions is small.

KAMEL (1987) presented an integral equation solution of the equations of the zeroth approximation and the first order perturbation for Rossby number. Figure 5 shows the variation of the concentration of suspended sediment along the

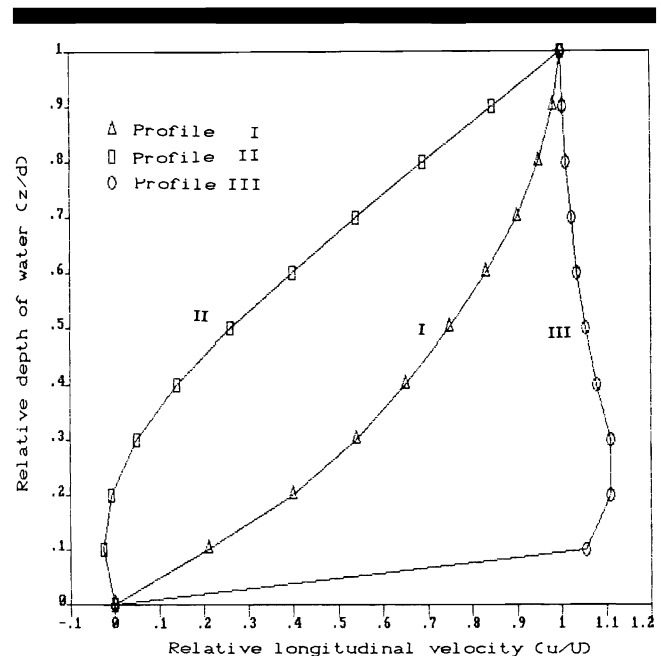


Figure 3. Types of the velocity profiles obtained from the solution of the zeroth approximation (Kamel, 1978).

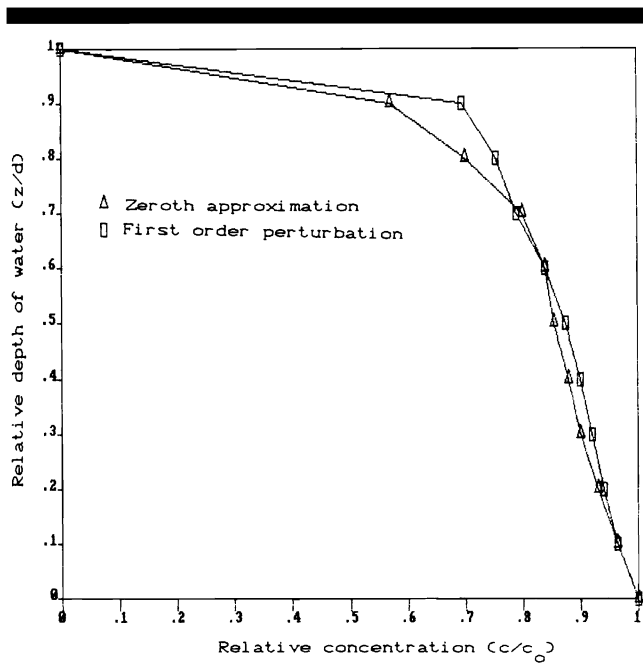


Figure 4. Comparison between the profiles of the relative concentration of suspended sediment obtained from the solution of the zeroth approximation and the first order perturbation for Rossby number (Kamel, 1978).

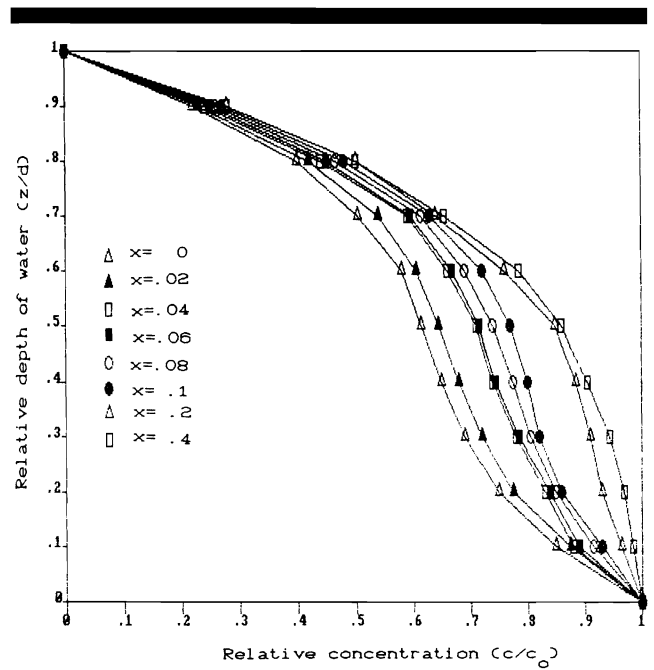


Figure 5. Profiles of the relative concentration of suspended sediment along the estuary; the zeroth approximation (Kamel, 1987).

estuary. Figure 6 shows the profiles of the concentration of suspended sediment, at  $x = 0.1$ , obtained from the solution of the zeroth approximation and the first order perturbation for Rossby number; here also the difference between the two solutions is small. The reason for the small difference between the solutions of the zeroth approximation and the first order perturbation for Rossby number is that the latter shows the effect of the inertia terms only which are neglected in the equations of the zeroth approximation. In addition, the equations of the zeroth approximation included the significant terms, consequently higher approximations resulted in little improvements on the solution obtained from the zeroth approximation. It is noted that Figures 1 and 2 show a larger difference between the profiles of the concentration of suspended sediment obtained from the solution of the zeroth and the first approximations than the difference shown in Figures 4 and 6. The reason is that Figure 2 shows the solution of the first approximation, which is the superposition of the linearly independent solutions of the first order perturbations for Rossby and Ekman numbers (MILLMAN and KELLER, 1969), while Figures 4 and 6 show the solution of the first order perturbation for Rossby number only.

**FORMULATION**

The following six assumptions are made: (1) there is no deposition of suspended sediment and there is no pick up, by the flow, of bottom sediment; (2) the settling velocity of the sediment particles is constant; (3) the effect of salinity on the sedimentation process is negligible; (4) the longitudinal velocities of the water particles and of the sediment particles

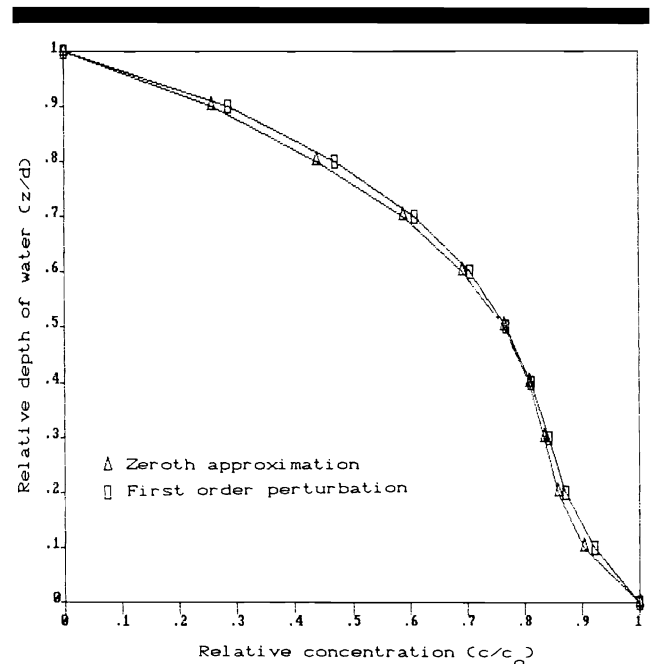


Figure 6. Comparison between the profiles of the relative concentration of suspended sediment obtained from the solution of the zeroth approximation and the first order perturbation for Rossby number (Kamel, 1987).

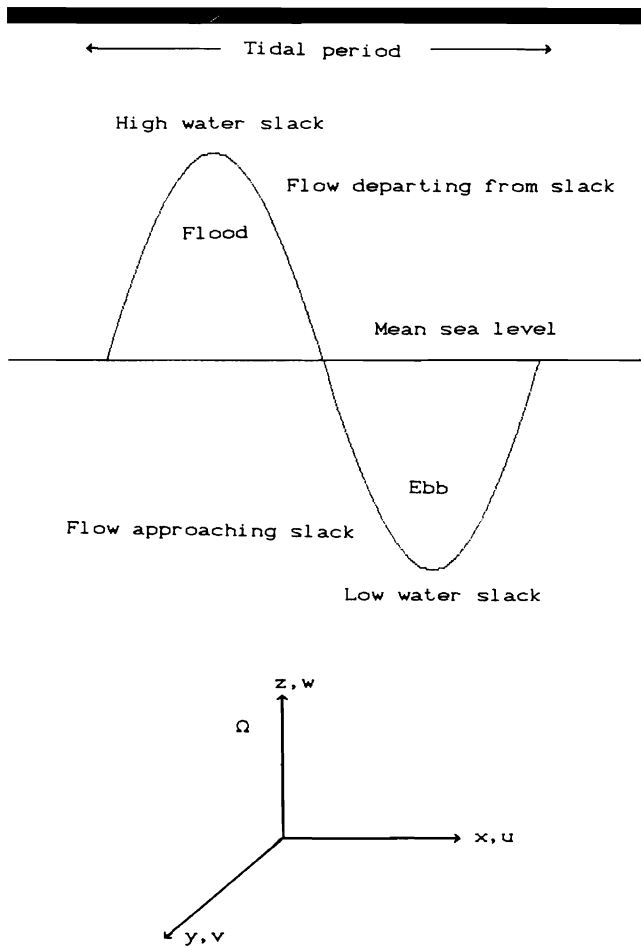


Figure 7. a and b. Definition sketches: (a) the tidal parameters, and (b) the system of coordinates used.

are equal; (5) the vertical velocity of the sediment particles is equal to the vertical velocity of the water particles plus the settling velocity of the sediment particles, and (6) the pressure is hydrostatic. The first assumption is justified since emphasis in this study is on the mechanics of sediment suspension without probing into the interaction between the flow and the bed. Assumption (2) is based on the postulate that the settling velocity of the sediment particles is independent of the concentration; the assumption is justified for small concentrations of sediment. Assumption (3) neglects the effect of density differences due to salinity. It is believed that in well mixed estuaries salinity has a small effect on the sedimentation process. Assumptions (4) and (5) could be justified provided that: (a) the size of the sediment particles is small compared with the length scales of turbulence; this is the case in estuaries where most of the suspended material is composed of fine constituents, and (b) the acceleration of the particles is small compared with the acceleration due to gravity; this is the case in estuarine flow since the tidal periods are long and also since the problem is formulated for flow near slack, Figure 7a, where the flow velocities and accelerations are

small. Assumption (6) is justified since the flow acceleration is small.

For a three dimensional flow with the axis  $ox$  horizontal, coinciding with the bottom of the estuary, the axis  $oz$  vertically upwards, and the axis  $oy$  perpendicular to the  $(x, z)$  plan, Figure 7b; the equations of conservation of volume, of mass, and of momentum, for shallow water, take the form, (PEDLOSKEY, 1987):

Equation of conservation of volume:

$$\frac{\partial u}{\partial x} + \frac{\partial v}{\partial y} + \frac{\partial w}{\partial z} = 0 \quad (1)$$

Equation of conservation of mass:

$$\frac{\partial \rho}{\partial t} + \frac{\partial(\rho u)}{\partial x} + \frac{\partial(\rho v)}{\partial y} + \frac{\partial(\rho w)}{\partial z} = 0 \quad (2)$$

Equation of conservation of momentum in the x-direction:

$$\rho \frac{Du}{Dt} - \rho fv = -\frac{\partial p}{\partial x} + \frac{\partial}{\partial x} \frac{\mu \partial u}{\partial x} + \frac{\partial}{\partial y} \frac{\mu \partial u}{\partial y} + \frac{\partial}{\partial z} \frac{\mu \partial u}{\partial z} \quad (3)$$

Equation of conservation of momentum in the y-direction:

$$\rho \frac{Dv}{Dt} + \rho fu = -\frac{\partial p}{\partial y} + \frac{\partial}{\partial x} \frac{\mu \partial v}{\partial x} + \frac{\partial}{\partial y} \frac{\mu \partial v}{\partial y} + \frac{\partial}{\partial z} \frac{\mu \partial v}{\partial z} \quad (4)$$

Equation of conservation of momentum in the z-direction:

$$\rho \frac{Dw}{Dt} = -\frac{\partial p}{\partial z} + \frac{\partial}{\partial x} \frac{\mu \partial w}{\partial x} + \frac{\partial}{\partial y} \frac{\mu \partial w}{\partial y} + \frac{\partial}{\partial z} \frac{\mu \partial w}{\partial z} \quad (5)$$

where

$$\frac{D}{Dt} \equiv \frac{\partial}{\partial t} + u \frac{\partial}{\partial x} + v \frac{\partial}{\partial y} + w \frac{\partial}{\partial z} \quad (6)$$

where  $g$  is the acceleration due to gravity;  $p$  is the pressure;  $u$ ,  $v$ , and  $w$  respectively are the longitudinal, the transverse, and the vertical velocities of the flow;  $x$ ,  $y$ , and  $z$  respectively, are the longitudinal, the transverse, and the vertical coordinates;  $t$  is the time;  $\rho$  is the density;  $\mu$  is the dynamic viscosity; and  $f$  is the Coriolis parameter.

To the above equations, the equation of kinetic energy of turbulence is added. This equation is obtained by multiplying the equation of conservation of momentum in the x-direction (eq. 3) by  $u$ , the equation of conservation of momentum in the y-direction (eq. 4) by  $v$ , and the equation of conservation of momentum in the z-direction (eq. 5) by  $w$ , adding the resulting three equations, expanding all terms and taking the time average, then subtracting the equation of kinetic energy of the mean flow. The equation of kinetic energy of conservation of momentum in the x-direction (eq. 3), taking the time average, then multiplying by  $u$ ; expanding the equation of conservation of momentum in the y-direction (eq. 4), taking the time average, then multiplying by  $v$ ; expanding the equation of conservation of momentum in the z-direction (eq. 5), taking

the time average, then multiplying by  $w$ ; then adding the above three equations; (TENNEKES and LUMELY, 1972).

$$\begin{aligned}
 & \text{advection} \\
 & \frac{1}{2} \frac{\partial(\bar{q}^2)}{\partial t} + \rho \left\{ \bar{u} \frac{\partial(\bar{u}'u')}{\partial x} + \bar{v} \frac{\partial(\bar{u}'v')}{\partial x} + \frac{1}{2} \bar{u} \frac{\partial(\bar{v}'v')}{\partial x} \right. \\
 & \quad + \frac{1}{2} \bar{u} \frac{\partial(\bar{w}'w')}{\partial x} + \bar{u} \frac{\partial(\bar{v}'v')}{\partial y} + \bar{w} \frac{\partial(\bar{w}'w')}{\partial y} \\
 & \quad + \frac{1}{2} \bar{v} \frac{\partial(\bar{u}'u')}{\partial y} + \bar{v} \frac{\partial(\bar{v}'v')}{\partial y} + \frac{1}{2} \bar{v} \frac{\partial(\bar{w}'w')}{\partial y} \\
 & \quad + \bar{u} \frac{\partial(\bar{w}'w')}{\partial z} + \bar{v} \frac{\partial(\bar{w}'w')}{\partial z} + \frac{1}{2} \bar{w} \frac{\partial(\bar{u}'u')}{\partial z} \\
 & \quad \left. + \frac{1}{2} \bar{w} \frac{\partial(\bar{v}'v')}{\partial z} + \bar{w} \frac{\partial(\bar{w}'w')}{\partial z} \right\} \\
 & \text{production} \\
 & + \rho \left\{ \frac{\partial(\bar{u}'u')\bar{u}}{\partial x} + \frac{\partial(\bar{u}'v')\bar{v}}{\partial x} + \frac{\partial(\bar{u}'w')\bar{w}}{\partial x} + \frac{\partial(\bar{u}'v')\bar{u}}{\partial y} \right. \\
 & \quad + \frac{\partial(\bar{v}'v')\bar{v}}{\partial y} + \frac{\partial(\bar{v}'w')\bar{w}}{\partial y} + \frac{\partial(\bar{u}'w')\bar{u}}{\partial z} \\
 & \quad \left. + \frac{\partial(\bar{v}'w')\bar{v}}{\partial z} + \frac{\partial(\bar{w}'w')\bar{w}}{\partial z} \right\} \\
 & \text{diffusion} \\
 & + \left\{ \left[ \frac{\partial(\bar{u}'p')}{\partial x} + \frac{\partial(\bar{u}'u')\bar{u}}{\partial x} + \frac{\partial(\bar{u}'v')\bar{v}}{\partial x} + \frac{\partial(\bar{u}'w')\bar{w}}{\partial x} \right] \right. \\
 & \quad + \left[ \frac{\partial(\bar{v}'p')}{\partial y} + \frac{\partial(\bar{u}'v')\bar{u}}{\partial y} + \frac{\partial(\bar{v}'v')\bar{v}}{\partial y} + \frac{\partial(\bar{v}'w')\bar{w}}{\partial y} \right] \\
 & \quad \left. + \left[ \frac{\partial(\bar{w}'p')}{\partial z} + \frac{\partial(\bar{u}'w')\bar{u}}{\partial z} + \frac{\partial(\bar{v}'w')\bar{v}}{\partial z} + \frac{\partial(\bar{w}'w')\bar{w}}{\partial z} \right] \right\} \\
 & \text{dissipation} \\
 & - \frac{1}{2} \left\{ \frac{\partial}{\partial x} \left[ \mu \frac{\partial(\bar{u}'u')}{\partial x} \right] + \frac{\partial}{\partial y} \left[ \mu \frac{\partial(\bar{u}'u')}{\partial y} \right] + \frac{\partial}{\partial z} \left[ \mu \frac{\partial(\bar{u}'u')}{\partial z} \right] \right. \\
 & \quad + \frac{\partial}{\partial x} \left[ \mu \frac{\partial(\bar{v}'v')}{\partial x} \right] + \frac{\partial}{\partial y} \left[ \mu \frac{\partial(\bar{v}'v')}{\partial y} \right] + \frac{\partial}{\partial z} \left[ \mu \frac{\partial(\bar{v}'v')}{\partial z} \right] \\
 & \quad \left. + \frac{\partial}{\partial x} \left[ \mu \frac{\partial(\bar{w}'w')}{\partial x} \right] + \frac{\partial}{\partial y} \left[ \mu \frac{\partial(\bar{w}'w')}{\partial y} \right] + \frac{\partial}{\partial z} \left[ \mu \frac{\partial(\bar{w}'w')}{\partial z} \right] \right\} \\
 & + \mu \left[ \frac{\partial(\bar{u}'u')^2}{\partial x} + \frac{\partial(\bar{u}'u')^2}{\partial y} + \frac{\partial(\bar{u}'u')^2}{\partial z} + \frac{\partial(\bar{v}'v')^2}{\partial x} + \frac{\partial(\bar{v}'v')^2}{\partial y} \right. \\
 & \quad \left. + \frac{\partial(\bar{v}'v')^2}{\partial z} + \frac{\partial(\bar{w}'w')^2}{\partial x} + \frac{\partial(\bar{w}'w')^2}{\partial y} + \frac{\partial(\bar{w}'w')^2}{\partial z} \right] = 0 \quad (7)
 \end{aligned}$$

where the superscripts “ $\bar{\quad}$ ” and “ $\bar{\quad}'$ ” respectively denote the

mean value and the fluctuation from the mean value, and  $q^2 = (\bar{u}'u') + (\bar{v}'v') + (\bar{w}'w')$ . In eqs. 1–7 terms which included the third moments ( $\bar{u}'u'_j u'_k$ ) were neglected.

For a two component flow which consists of a mixture of water and sediment, the equations of conservation of volume, of mass, and of momentum, and the equation of kinetic energy of turbulence (eqs. 8–13) are obtained from eqs. 1, 2, 3, 4, 5 and 7 as follows. The equation of conservation of volume (eq. 1) remains unchanged and is given a new number as eq. 8. The equation of conservation of mass (eq. 9) is obtained from eq. 2 by replacing the density  $\rho$  once by  $(1 - c)\rho_w$  and once by  $c\rho_s$ , where  $c$  is the concentration of suspended sediment by volume, and the subscripts “s” and “w” respectively, denote sediment and water. The resulting two equations are added, each term is expressed by its mean value and its fluctuating component and the time average of all terms is taken. Similarly, each of the three equations of linear momentum (eqs. 10–12) are obtained from eqs. 3–5 by replacing the density  $\rho$  once by  $(1 - c)\rho_w$  and once by  $c\rho_s$ . The resulting two equations are added, each term is expressed by its mean value and its fluctuating component, and the time average of all terms is taken. The equation of kinetic energy of turbulence (eq. 13) is obtained as follows: multiplying the equation of conservation of momentum in the x-direction (eq. 3) by  $u$ , the equation of conservation of momentum in the y-direction (eq. 4) by  $v$ , and the equation of conservation of momentum in the z-direction (eq. 5) by  $w$ , and adding the resulting three equations; in the resulting equations the density  $\rho$  is replaced once by  $(1 - c)\rho_w$  and once by  $c\rho_s$  and the resulting two equations are added, each term is expressed by its mean value and its fluctuating component and the time average of all terms is taken, then subtracting the equation of kinetic energy of the mean flow for a two component flow. The equation of kinetic energy of the mean flow for a two component flow is obtained from the equation of kinetic energy of the mean flow by replacing the density  $\rho$  once by  $(1 - c)\rho_w$  and once by  $c\rho_s$  then adding the resulting two equations (VASELIEV, 1969).

Because flow in estuaries is essentially two dimensional except for turbulence which is strongly three dimensional, the changes in the y-direction could be neglected except for terms representing turbulence, *i.e.* fluctuating terms. Therefore setting  $v = 0$ ,  $\partial(c, p, u, w)/\partial z = 0$ , and dropping over bars for convenience, eqs. 1, 2, 3, 4, 5, and 7 for a two component flow take the form given by eqs. 8–13. In eqs. 8–13  $w$  is the settling velocity of the sediment particles and the viscosity of the mixture ( $\mu_m$ ) is expressed as:  $\mu_m = \mu_w(1 + 2.5c)$ .

Equation of conservation of volume:

$$\frac{\partial u}{\partial x} + \frac{\partial w}{\partial z} = 0 \quad (8)$$

Equation of conservation of mass:

$$\begin{aligned}
 \frac{\partial c}{\partial t} + u \frac{\partial c}{\partial x} + w \frac{\partial c}{\partial z} - \left[ \frac{\rho_s}{(\rho_s - \rho_w)} \dot{w} \right] \frac{\partial c}{\partial z} \\
 + \frac{\partial(\bar{c}'u')}{\partial x} + \frac{\partial(\bar{c}'v')}{\partial y} + \frac{\partial(\bar{c}'w')}{\partial z} = 0 \quad (9)
 \end{aligned}$$

Equation of conservation of momentum in the x-direction:

$$\begin{aligned} & \frac{\partial\{(1-c)\rho_w + c\rho_s\}u}{\partial t} + \frac{\partial\{(1-c)\rho_w + c\rho_s\}uw}{\partial x} \\ & + \frac{\partial\{(1-c)\rho_w + c\rho_s\}uw}{\partial z} - \frac{\partial(\rho_s \dot{w}cu)}{\partial z} \\ & - (\rho_s - \rho_w)g \sin \theta c + (\rho_s - \rho_w)g \cos \theta \int \frac{\partial c}{\partial x} dz \\ & - \left\{ \frac{\partial\left[(1+2.5c)\mu_w \frac{\partial u}{\partial x}\right]}{\partial x} + \frac{\partial\left[(1+2.5c)\mu_w \frac{\partial u}{\partial z}\right]}{\partial z} \right\} \\ & + \frac{\partial\{(1-c)\rho_w + c\rho_s\}(\overline{u'u'})}{\partial x} + \frac{\partial\{(1-c)\rho_w + c\rho_s\}(\overline{u'v'})}{\partial y} \\ & + \frac{[(1-c)\rho_w + c\rho_s]\partial(\overline{w'w'})}{\partial z} = 0 \end{aligned} \tag{10}$$

Equation of conservation of momentum in the y-direction:

$$\begin{aligned} & f\{(1-c)\rho_w + c\rho_s\}u + \frac{\partial\{(1-c)\rho_w + c\rho_s\}(\overline{u'v'})}{\partial x} \\ & + \frac{\partial\{(1-c)\rho_w + c\rho_s\}(\overline{v'v'})}{\partial y} + \frac{[(1-c)\rho_w + c\rho_s]\partial(\overline{v'w'})}{\partial z} = 0 \end{aligned} \tag{11}$$

Equation of conservation of momentum in the z-direction:

$$\begin{aligned} & \frac{\partial\{(1-c)\rho_w + c\rho_s\}w}{\partial t} + \frac{\partial\{(1-c)\rho_w + c\rho_s\}uw}{\partial x} \\ & + \frac{\partial\{(1-c)\rho_w + c\rho_s\}ww}{\partial z} - \frac{\partial(\rho_s \dot{w}cu)}{\partial x} \\ & + \frac{\partial(\rho_s c \dot{w}^2)}{\partial z} - \frac{\partial(2\rho_s \dot{w}cw)}{\partial z} + (\rho_s - \rho_w)gc \\ & - \left\{ \frac{\partial\left[(1+2.5c)\mu_w \frac{\partial w}{\partial x}\right]}{\partial x} + \frac{\partial\left[(1+2.5c)\mu_w \frac{\partial w}{\partial z}\right]}{\partial z} \right\} \\ & + \frac{\partial\{(1-c)\rho_w + c\rho_s\}(\overline{u'w'})}{\partial x} + \frac{\partial\{(1-c)\rho_w + c\rho_s\}(\overline{v'w'})}{\partial y} \\ & + [(1-c)\rho_w + c\rho_s] \frac{\partial(\overline{w'w'})}{\partial z} = 0 \end{aligned} \tag{12}$$

Equation of kinetic energy of turbulence:

$$\begin{aligned} & \frac{1}{2}[(1-c)\rho_w + c\rho_s] \frac{\partial(\overline{q^2})}{\partial t} \\ & + \left\{ \begin{array}{l} \text{advection} \\ [(1-c)\rho_w + c\rho_s] \left[ u \frac{\partial(\overline{u'u'})}{\partial x} + \frac{1}{2}u \frac{\partial(\overline{v'v'})}{\partial x} \right. \right. \\ \left. \left. + \frac{1}{2}u \frac{\partial(\overline{w'w'})}{\partial x} + u \frac{v'\partial u'}{\partial y} \right. \right. \\ \left. \left. + w \frac{v'\partial w'}{\partial y} + u \frac{w'\partial u'}{\partial z} \right] \right\} \end{aligned}$$

$$\begin{aligned} & + \frac{1}{2}w \frac{\partial(\overline{u'u'})}{\partial z} + \frac{1}{2}w \frac{\partial(\overline{v'v'})}{\partial z} \\ & + w \frac{\partial(\overline{w'w'})}{\partial z} \left. \right\} \end{aligned}$$

production

$$\begin{aligned} & + \left\{ [(1-c)\rho_w + c\rho_s] \left[ (\overline{u'u'}) \frac{\partial u}{\partial x} + (\overline{u'w'}) \frac{\partial w}{\partial x} \right. \right. \\ & \left. \left. + \frac{(\overline{u'w'})\partial u}{\partial z} + \frac{(\overline{w'w'})\partial w}{\partial z} \right] \right\} \end{aligned}$$

diffusion

$$\begin{aligned} & + \left\{ \left[ \frac{\partial(\overline{u'p'})}{\partial x} + \frac{\partial(\overline{v'p'})}{\partial y} + \frac{\partial(\overline{w'p'})}{\partial z} \right] \right. \\ & + [(1-c)\rho_w + c\rho_s] \left[ \frac{(\overline{u'u'})\partial u'}{\partial x} + \frac{(\overline{u'v'})\partial v'}{\partial x} \right. \\ & \left. + \frac{(\overline{u'w'})\partial w'}{\partial x} + \frac{(\overline{v'v'})\partial v'}{\partial y} + \frac{(\overline{v'w'})\partial w'}{\partial y} \right. \\ & \left. + \frac{(\overline{u'w'})\partial u'}{\partial z} + \frac{(\overline{v'w'})\partial v'}{\partial z} \right. \\ & \left. \left. + \frac{(\overline{w'w'})\partial w'}{\partial z} \right] \right\} \end{aligned}$$

suspension

$$\begin{aligned} & + \left\{ (\rho_s - \rho_w) \left[ -(\overline{c'u'})g \sin \theta \right. \right. \\ & \left. \left. + \frac{1}{2}g \cos \theta \int \left( \frac{\partial(\overline{c'u'})}{\partial x} \right) dz + (\overline{c'w'})g \right] \right\} \end{aligned}$$

dissipation

$$\begin{aligned} & - \frac{1}{2} \left\{ \frac{\partial\left[(1+2.5c)\mu_w \frac{\partial(\overline{u'u'})}{\partial x}\right]}{\partial x} + (1+2.5c)\mu_w \frac{\partial^2(\overline{u'u'})}{\partial y^2} \right. \\ & \left. + \frac{\partial\left[(1+2.5c)\mu_w \frac{\partial(\overline{u'u'})}{\partial z}\right]}{\partial z} + \frac{\partial\left[(1+2.5c)\mu_w \frac{\partial(\overline{v'v'})}{\partial x}\right]}{\partial x} \right. \\ & \left. + (1+2.5c)\mu_w \frac{\partial^2(\overline{v'v'})}{\partial y^2} + \frac{\partial\left[(1+2.5c)\mu_w \frac{\partial(\overline{v'v'})}{\partial z}\right]}{\partial z} \right. \\ & \left. + \frac{\partial\left[(1+2.5c)\mu_w \frac{\partial(\overline{w'w'})}{\partial x}\right]}{\partial x} + (1+2.5c)\mu_w \frac{\partial^2(\overline{w'w'})}{\partial y^2} \right. \\ & \left. + \frac{\partial\left[(1+2.5c)\mu_w \frac{\partial(\overline{w'w'})}{\partial z}\right]}{\partial z} \right\} \end{aligned}$$

$$\begin{aligned}
 & + \left\{ (1 + 2.5c)\mu_w \left[ \overline{\left(\frac{\partial u'}{\partial x}\right)^2} + \overline{\left(\frac{\partial u'}{\partial y}\right)^2} + \overline{\left(\frac{\partial u'}{\partial z}\right)^2} \right] \right. \\
 & + \overline{\left(\frac{\partial v'}{\partial x}\right)^2} + \overline{\left(\frac{\partial v'}{\partial y}\right)^2} + \overline{\left(\frac{\partial v'}{\partial z}\right)^2} \\
 & \left. + \overline{\left(\frac{\partial w'}{\partial x}\right)^2} + \overline{\left(\frac{\partial w'}{\partial y}\right)^2} + \overline{\left(\frac{\partial w'}{\partial z}\right)^2} \right\} = 0 \tag{13}
 \end{aligned}$$

The terms  $-(\rho_s - \rho_w)g \sin \theta c + (\rho_s - \rho_w)g \cos \theta \int (\partial c/\partial x) dz$  introduced in the equation of conservation of momentum in the x-direction (eq. 10) and appearing as  $-(\rho_s - \rho_w)(c'u')g \sin \theta + (1/2)(\rho_s - \rho_w)g \cos \theta \int [\partial(c'u')/\partial x] dz$  in the equation of kinetic energy of turbulence (eq. 13) represent the effect of excessive density by considering deriving forces consisting of gravity and pressure gradient. The gravity term  $(\rho_s - \rho_w)gc$ , introduced in the equation of conservation of momentum in the z-direction (eq. 12) and appearing as  $(\rho_s - \rho_w)(c'w')g$  in the equation of kinetic energy of turbulence (eq. 13), assumes that sediment loads in the water behave as a solid body. This would make the magnitude of these two terms considerably larger than the other gravity terms after eqs. 12 and 13 are closed and expressed in dimensionless form. The gravity terms would have the same order of magnitude by making  $g$  dimensionless as  $g(g)$  in the terms  $\{[-(\rho_s - \rho_w)g \sin \theta c + (\rho_s - \rho_w)g \cos \theta \int (\partial c/\partial x) dz], [-(\rho_s - \rho_w)(c'u')g \sin \theta + (1/2)(\rho_s - \rho_w)g \cos \theta \int [\partial(c'u')/\partial x] dz]\}$ , and by making  $g$  dimensionless as  $(L^2/g)$  in the terms  $\{[(\rho_s - \rho_w)gc], [(\rho_s - \rho_w)(c'w')g]\}$  as given later in section V—expressing the equations in dimensionless form.

**CLOSURE**

The six eqs. 8–13 contain the following unknowns: (1) the unknowns  $c$ ,  $u$ , and  $w$ ; (2) unknowns caused by the presence of terms representing the fluctuations in the concentration of suspended sediment ( $c'$ ) and their space derivatives, *i.e.*:  $(c'u'_i)$ , and  $u'_i(\partial c'/\partial x_j)$ ; (3) unknowns caused by the presence of terms representing fluctuations of the flow field, *i.e.*:  $(u'_i u'_j)$ , the second moments of the velocity fluctuations and their space derivatives  $(u'_i u'_j / \partial x_k)$ ,  $(\partial u'_i / \partial x_j)^2$ ; and the third moments of the velocity fluctuations and their space derivatives  $(u'_i u'_j \partial u'_k / \partial x_l)$ ; and (4) unknowns caused by the presence of terms representing fluctuations in the pressure field ( $p'$ ), *i.e.*:  $(u'_i p')$ .

The number of unknowns is reduced to the number of equations as follows: (i) the semi-empirical theories of turbulence presented by MONIN and YAGLOM (1971) are used for the closure of the terms representing concentration and velocity fluctuations appearing in the equation of conservation of mass and in the suspension term of the equation of kinetic energy of turbulence:

$$\overline{(c'u')} = -\epsilon \left(\frac{\partial c}{\partial x}\right), \quad (c'v') = -\epsilon \left(\frac{\partial c}{\partial y}\right) \quad \text{and} \quad \overline{(c'w')} = -\epsilon \left(\frac{\partial c}{\partial z}\right) \tag{14}$$

where  $\epsilon$  is the coefficient of exchange of mass. (2) The experimental data of Tennekes and Lumely (1972) could be used

to close the terms representing velocity fluctuations appearing in the equations of conservation of momentum and in the advection, production, and dissipation terms of the equation of kinetic energy of turbulence:

$$-\overline{(u'w')} = u_*^2, \quad \overline{(u'u')} \cong 4u_*^2, \quad \overline{(w'w')} = 0.64u_*^2 \tag{15}$$

where  $u_*$  is the shear velocity, a function of the water depth; the wall shear velocity is denoted by  $u_{*0}$ . The above relationships are only valid in the inertial sub layer, *i.e.*  $(z/d) \ll 1$ . Lacking similar experimental relationships for the core region, the terms representing velocity fluctuations are closed using the core region approximation of Tennekes and Lumely (1972) as follows:

$$\overline{(u'u')} = -\overline{(v'v')} = \overline{(w'w')} = 0.64u_*^2,$$

and

$$-\overline{(u'v')} = -\overline{(u'w')} = -\overline{(v'w')} = u_*^2 \tag{16}$$

Herein,  $u_*^2 = (\tau/\rho)$  and  $u_{*0}^2 = (\tau_0/\rho)$  where  $\tau$  is the turbulent shear stress, a function of the water depth, and  $\tau_0$  is the turbulent shear stress at the wall. (3) Terms representing velocity fluctuations and their space derivatives in the form  $(u'_i \partial u'_j / \partial x_k)$  which are part of the advection term are closed as:  $\partial(\alpha u_*^2) / \partial x_k$ , where  $\alpha$  is a numerical constant, *e.g.*,

$$\left(\frac{u' \partial u'}{\partial x}\right) = \frac{1}{2} \frac{\partial(\overline{u'u'})}{\partial x} = \frac{1}{2} \frac{\partial(0.64u_*^2)}{\partial x} = 0.32 \frac{\partial u_*^2}{\partial x} \tag{17}$$

(4) In the advection term,  $\bar{q}2$  is closed as:  $\bar{q}2 = (\tau/a\rho)$ ,  $a = 0.52$  (BRADSHAW *et al.*, 1967). (5) The diffusion term is closed as in (BRADSHAW *et al.*, 1967):

$$\left\{ \frac{p'w'}{\rho} + \frac{1}{2}(q2w') \right\} = G \left[ \left(\frac{\tau_{\max}}{\rho}\right)^{1/2} \left(\frac{\tau}{\rho}\right) \right] \tag{18}$$

The function  $G$  is approximated as:

$$G = \left(\frac{\tau_{\max}}{\rho U_1^2}\right)^{1/2} \left[ 5.333 \left(\frac{z}{\delta}\right) - 9 \left(\frac{z}{\delta}\right)^2 + 36.66 \left(\frac{z}{\delta}\right)^3 \right] \tag{19}$$

where  $U_1$  is the outer velocity and is equal to unity; herein  $U_1 \equiv U$ . (6) In the dissipation term,  $\nu(\partial u'_i / \partial x_j)^2 (\equiv E)$  is closed as in BRADSHAW *et al.* (1967):

$$E = \left(\frac{\tau}{\rho}\right)^{3/2} \mathbb{L}^{-1} \tag{20}$$

where  $\nu$  is the kinematic viscosity, and  $\mathbb{L}$  is a dissipation length parameter which varies as  $\kappa z$  near the wall and  $\kappa$  is von Karman's constant.  $\mathbb{L}$  is expressed as:

$$\frac{\mathbb{L}}{\delta} \cong 0.4 \left(\frac{z}{\delta}\right) + 0.2079 \left(\frac{z}{\delta}\right)^2 - 1.9475 \left(\frac{z}{\delta}\right)^3 + 1.3792 \left(\frac{z}{\delta}\right)^4 \tag{21}$$

where  $\delta$  is the thickness of the boundary layer and is equal to 1. Eq. 21 shows that for small values of  $z$ , the dissipation length parameter  $\mathbb{L}$  reduces to the mixing length  $\ell = \kappa z$  where  $\kappa = 0.4$ .

The closure of BRADSHAW *et al.* (1967), used above is based

on the reasoning that the shear stress profile is more closely related to the parameters describing the turbulence structure than to the mean velocity profile; e.g. the turbulent intensity is related to the local shear stress, the dissipation rate is related to the local shear stress and a dissipation length parameter which is a function of  $(z/\delta)$ , and the energy diffusion is related to the local shear stress and the maximum value of the shear stress [Figure 2 of BRADSHAW *et al.* (1967)].

Affecting the closures given by eqs. 14–21, the closed form of eqs. 8–13 is given as:

Equation of conservation of volume:

$$\frac{\partial u}{\partial x} + \frac{\partial w}{\partial z} = 0 \quad (8) \text{ bis}$$

Equation of conservation of mass:

$$\begin{aligned} \frac{\partial c}{\partial t} + u \frac{\partial c}{\partial x} + w \frac{\partial c}{\partial z} - \left[ \frac{\rho_s}{(\rho_s - \rho_w)} \dot{w} \frac{\partial c}{\partial z} \right. \\ \left. - \frac{\partial \left( \epsilon \frac{\partial c}{\partial x} \right)}{\partial x} - \frac{\partial \left( \epsilon \frac{\partial c}{\partial y} \right)}{\partial y} - \frac{\partial \left( \epsilon \frac{\partial c}{\partial z} \right)}{\partial z} \right] = 0 \end{aligned} \quad (22)$$

Equation of conservation of momentum in the x-direction:

$$\begin{aligned} \frac{\partial \{[(1-c)\rho_w + c\rho_s]u\}}{\partial t} + \frac{\partial \{[(1-c)\rho_w + c\rho_s]uw\}}{\partial x} \\ + \frac{\partial \{[(1-c)\rho_w + c\rho_s]uw\}}{\partial z} - \frac{\partial(\rho_s \dot{w}cu)}{\partial z} \\ - \left[ (\rho_s - \rho_w)g \sin \theta c - (\rho_s - \rho_w)g \cos \theta \int \left( \frac{\partial c}{\partial x} \right) dz \right] \\ - \left\{ \frac{\partial \left[ (1+2.5c)\mu_w \frac{\partial u}{\partial x} \right]}{\partial x} + \frac{\partial \left[ (1+2.5c)\mu_w \frac{\partial u}{\partial z} \right]}{\partial z} \right\} \\ + 0.64 \frac{\partial \tau}{\partial x} - \frac{\partial \tau}{\partial y} - \frac{\partial \tau}{\partial z} = 0 \end{aligned} \quad (23)$$

Equation of conservation of momentum in the y-direction:

$$f[(1-c)\rho_w + c\rho_s]u - \frac{\partial \tau}{\partial x} + 0.64 \frac{\partial \tau}{\partial y} - \frac{\partial \tau}{\partial z} = 0 \quad (24)$$

Equation of conservation of momentum in the z-direction:

$$\begin{aligned} \frac{\partial \{[(1-c)\rho_w + c\rho_s]w\}}{\partial t} + \frac{\partial \{[(1-c)\rho_w + c\rho_s]uw\}}{\partial x} \\ + \frac{\partial \{[(1-c)\rho_w + c\rho_s]ww\}}{\partial z} - \frac{\partial(\rho_s \dot{w}cw)}{\partial x} \\ - \frac{\partial(\rho_s c \dot{w}^2)}{\partial z} - \frac{\partial(2\rho_s \dot{w}cw)}{\partial z} + [(\rho_s - \rho_w)gc] \\ - \left\{ \frac{\partial \left[ (1+2.5c)\mu_w \frac{\partial w}{\partial x} \right]}{\partial x} + \frac{\partial \left[ (1+2.5c)\mu_w \frac{\partial w}{\partial z} \right]}{\partial z} \right\} \\ - \frac{\partial \tau}{\partial x} - \frac{\partial \tau}{\partial y} + 0.64 \frac{\partial \tau}{\partial z} = 0 \end{aligned} \quad (25)$$

Equation of kinetic energy of turbulence:

$$\begin{aligned} \frac{1}{2} [(1-c)\rho_w + c\rho_s] \frac{\partial \left( \frac{\tau}{\rho} \right)}{\partial t} \\ \text{advection} \\ + \left\{ [(1-c)\rho_w + c\rho_s] \left[ \frac{1}{2} u \frac{\partial \left( \frac{\tau}{\rho} \right)}{\partial x} + \frac{1}{2} w \frac{\partial \left( \frac{\tau}{\rho} \right)}{\partial z} \right. \right. \\ \left. \left. + 0.32u \frac{\partial \left( \frac{\tau}{\rho} \right)}{\partial x} + 0.32w \frac{\partial \left( \frac{\tau}{\rho} \right)}{\partial z} \right. \right. \\ \left. \left. - \frac{1}{2} u \frac{\partial \left( \frac{\tau}{\rho} \right)}{\partial y} - \frac{1}{2} w \frac{\partial \left( \frac{\tau}{\rho} \right)}{\partial y} \right. \right. \\ \left. \left. - \frac{1}{2} u \frac{\partial \left( \frac{\tau}{\rho} \right)}{\partial z} \right] \right\} \\ \text{production} \\ + \left\{ [(1-c)\rho_w + c\rho_s] \left[ 0.64 \left( \frac{\tau}{\rho} \right) \frac{\partial u}{\partial x} - \left( \frac{\tau}{\rho} \right) \frac{\partial w}{\partial x} \right. \right. \\ \left. \left. - \left( \frac{\tau}{\rho} \right) \frac{\partial u}{\partial z} + 0.64 \left( \frac{\tau}{\rho} \right) \frac{\partial w}{\partial z} \right] \right\} \\ \text{diffusion} \\ + \left\{ \left( \frac{\partial}{\partial x} + \frac{\partial}{\partial y} + \frac{\partial}{\partial z} \right) \right. \\ \left. \left[ \tau \frac{\tau_{\max}}{\rho U_1} \left[ 5.333 \left( \frac{z}{\delta} \right) - 9 \left( \frac{z}{\delta} \right)^2 + 36.667 \left( \frac{z}{\delta} \right)^3 \right] \right] \right\} \\ \text{suspension} \\ + \left\{ (\rho_s - \rho_w)g \sin \theta \left( \epsilon \frac{\partial c}{\partial x} \right) \right. \\ \left. - \frac{1}{2} (\rho_s - \rho_w)g \cos \theta \int \left[ \frac{\partial \left( \epsilon \frac{\partial c}{\partial x} \right)}{\partial x} \right] dz \right. \\ \left. - (\rho_s - \rho_w)g \left( \epsilon \frac{\partial c}{\partial z} \right) \right\} \\ \text{dissipation} \\ + \left\{ \left[ \tau \left( \frac{\tau}{\rho} \right)^{1/2} \right] \left[ 0.4\delta \left( \frac{z}{\delta} \right) + 0.2079\delta \left( \frac{z}{\delta} \right)^2 \right] \right\} \end{aligned}$$

$$\begin{aligned}
& - 1.9475\delta \left( \frac{z}{\delta} \right)^3 + 1.3792\delta \left( \frac{z}{\delta} \right)^4 \Big]^{-1} \Big\} \\
& - 0.96\mu_w \left\{ \partial \left[ \frac{(1 + 2.5c)\partial \left( \frac{\tau}{\rho} \right)}{\partial x} \right] (\partial x)^{-1} + (1 + 2.5c) \frac{\partial^2 \left( \frac{\tau}{\rho} \right)}{\partial y^2} \right\} \\
& + \partial \left[ \frac{(1 + 2.5c)\partial \left( \frac{\tau}{\rho} \right)}{\partial z} \right] (\partial z)^{-1} = 0 \quad (26)
\end{aligned}$$

### EXPRESSING THE EQUATIONS IN DIMENSIONLESS FORM

The physical data of the Delaware estuary, U.S.A. presented by EAGLESON (1966), and by KAMEL (1972) is adopted. Maximum tidal amplitude  $A = 1.67$  (m), average water depth in estuary  $d = 6.41$  (m), length of estuary  $L = 1.438 \times 10^5$  (m), average width of estuary  $W = 1,463$  (m), maximum longitudinal velocity  $U_{\max} = 0.67$  (m/s), maximum water surface slope  $S_{\max} = 2.17 \times 10^{-5}$ , Manning's coefficient of roughness  $n = 0.024$ , depth averaged longitudinal velocity for ebb flow departing from slack  $\bar{U} = 0.0305$  (m/s), average water surface slope for ebb flow departing from slack  $S = 4.49 \times 10^{-8}$ , maximum concentration of suspended sediment by volume  $c_0 = 10\%$ ,  $\rho_w = 10^3$  (kg/m<sup>3</sup>), and  $v_w = 1.18 \times 10^{-6}$  (m<sup>2</sup>/s). With  $\rho_{\max} = [(1 - c_0)\rho_w + c_0\rho_s] = 1.165 \rho_w$  (kg/m<sup>3</sup>), the maximum difference between the densities of the water-sediment mixture and that of water  $\Delta\rho = 0.165 \times 10^3$  (kg/m<sup>3</sup>). The maximum turbulent shear stress for ebb flow departing from slack is expressed as  $\tau_{\max} = \rho_{\max} g W S$  and is computed to be equal to 0.75 (kg/m s<sup>2</sup>). The maximum coefficient of exchange of mass given by EAGLESON (1966), following an analysis by G. I. Taylor for longitudinal dispersion in a straight pipe, could be expressed as  $\epsilon_{\max} = 63.33 (n/R^{1/6}) \bar{U} R$ , where  $R$  is the hydraulic radius of the estuary and is taken to be equal to the average water depth in the estuary  $d$ . For ebb flow departing from slack  $\epsilon_{\max}$  is computed to be equal to 0.218 (m<sup>2</sup>/s).

To reduce eqs. 8, 22, 23, 24, 25, and 26 to dimensionless form, let  $f^{-1}$ ,  $L$ ,  $R$ ,  $W$ ,  $\bar{U}$ ,  $\tau_{\max}$ ,  $\epsilon_{\max}$ ,  $\rho$ ,  $\Delta\rho$ , and  $\mu_w$  characterize respectively, the typical time, the horizontal length, the vertical length, the transverse length, the depth averaged longitudinal velocity for ebb flow departing from slack, the maximum shear stress for ebb flow departing from slack, the maximum coefficient of exchange of mass for ebb flow departing from slack, the density of the mixture of water and sediment, the maximum difference between the densities of the water-sediment mixture and that of water, and the dynamic viscosity of water. Replacing the variables  $f$ ,  $x$ ,  $y$ ,  $z$ ,  $u$ ,  $w$ ,  $\dot{w}$ ,  $\tau$ ,  $\epsilon$ ,  $\rho$ ,  $c$ ,  $\mu$ , and  $g$  by their scaled counterparts  $f(f)$ ,  $(L)x$ ,  $(W)y$ ,  $(R)z$ ,  $(\bar{U})u$ ,  $(R\bar{U}/L)w$ ,  $(\bar{U})\dot{w}$ ,  $(\tau_{\max})\tau$ ,  $(\epsilon_{\max})\epsilon$ ,  $(\rho_w)\rho$ ,  $(\Delta\rho/\rho)c$ ,  $(\mu_w)\mu$ , and  $(g)g$ , the dimensionless form of eqs. 8, 22, 23, 24, 25, and 26 is given, after a little algebraic manipulation, by eqs. 8, 27, 28, 29, 30, and 31 which are for steady state con-

ditions since the intention is to present the steady state solution of the problem.

Equation of conservation of volume:

$$\frac{\partial u}{\partial x} + \frac{\partial w}{\partial z} = 0 \quad (8) \text{ bis}$$

Equation of conservation of mass:

$$\begin{aligned}
\frac{\partial \left( \epsilon \frac{\partial c}{\partial z} \right)}{\partial z} + \frac{\rho_s}{\rho_s - \rho_w} \dot{w} \frac{\partial c}{\partial z} = \frac{R}{L} \left\{ u \frac{\partial c}{\partial x} + w \frac{\partial c}{\partial z} - \frac{\partial \left( \epsilon \frac{\partial c}{\partial y} \right)}{\partial y} \right\} \\
- E \left\{ \frac{\partial \left( \epsilon \frac{\partial c}{\partial x} \right)}{\partial x} \right\} \quad (27)
\end{aligned}$$

Equation of conservation of momentum in the x-direction:

$$\begin{aligned}
(\rho_s - \rho_w)g \cos \theta \int \frac{\partial c}{\partial x} dz - \rho_s \dot{w} \frac{\partial(cu)}{\partial z} - \frac{\partial \tau}{\partial z} \\
= \frac{R}{W} \frac{\partial \tau}{\partial y} + \left\{ \frac{\Delta\rho}{\rho} g \frac{R}{\bar{U}^2} \right\} (\sin \theta) \{ (\rho_s - \rho_w)gc \} \\
- \frac{R}{L} \left\{ \rho_w \frac{\partial(uu)}{\partial x} + (\rho_s - \rho_w) \frac{\partial(cuu)}{\partial x} + \rho_w \frac{\partial(uw)}{\partial z} \right. \\
\left. + (\rho_s - \rho_w) \frac{\partial(cuw)}{\partial z} + \frac{\partial \tau}{\partial x} \right\} \\
+ \frac{v_w}{\bar{U}R} \left\{ \mu_w \frac{\partial^2 u}{\partial z^2} + 2.5\mu_w \frac{\partial \left( c \frac{\partial u}{\partial z} \right)}{\partial z} \right\} \\
+ \frac{v_w}{\bar{U}R} \left( \frac{R}{L} \right)^2 \left\{ \mu_w \frac{\partial^2 u}{\partial x^2} + 2.5\mu_w \frac{\partial \left( c \frac{\partial u}{\partial x} \right)}{\partial x} \right\} \quad (28)
\end{aligned}$$

Equation of conservation of momentum in the y-direction:

$$\frac{\partial \tau}{\partial y} - \frac{\partial \tau}{\partial z} + [\rho_w + (\rho_s - \rho_w)c] fu = \frac{R}{L} \frac{\partial \tau}{\partial x} \quad (29)$$

Equation of conservation of momentum in the z-direction:

$$\begin{aligned}
(\rho_s - \rho_w)gc + \rho_s \dot{w}^2 \frac{\partial c}{\partial z} + \frac{\partial \tau}{\partial z} \\
= \frac{\tau_{\max} R}{\rho \bar{U}^2 W} \frac{\partial \tau}{\partial y} + \frac{R}{L} \left\{ \rho_s \dot{w} \frac{\partial(cu)}{\partial x} + 2\rho_s \dot{w} \frac{\partial(cw)}{\partial z} \right\} \\
+ \frac{\tau_{\max} R}{\rho \bar{U}^2 L} \frac{\partial \tau}{\partial x} - \left( \frac{R}{L} \right)^2 \left\{ \rho_w \frac{\partial(uw)}{\partial x} + (\rho_s - \rho_w) \frac{\partial(cuw)}{\partial x} \right. \\
\left. + \rho_w \frac{\partial(ww)}{\partial z} + (\rho_s - \rho_w) \frac{\partial(cww)}{\partial z} \right\}
\end{aligned}$$

$$\begin{aligned}
& -\frac{\nu_w R}{\mathbb{U}R L} \left( \mu_w \frac{\partial^2 w}{\partial z^2} + 2.5 \mu_w \frac{\partial \left( c \frac{\partial w}{\partial z} \right)}{\partial z} \right) \\
& + \left( \frac{\nu_w}{\mathbb{U}R} \right) \left( \frac{R}{L} \right)^2 \left( \mu_w \frac{\partial^2 w}{\partial x^2} + 2.5 \mu_w \frac{\partial \left( c \frac{\partial w}{\partial x} \right)}{\partial x} \right) \quad (30) \\
& + \left( \frac{R}{L} \right)^2 \left( \frac{\nu_w}{\mathbb{U}R} \right) \left\{ \frac{\mu_w}{\rho} \frac{\partial^2 \tau}{\partial x^2} + \frac{\mu_w}{\rho} \frac{\partial}{\partial x} \left[ c \frac{\partial \left( \frac{\tau}{\rho} \right)}{\partial x} \right] (\partial x) \right\}^2 \quad (31)
\end{aligned}$$

Equation of kinetic energy of turbulence:

$$\begin{aligned}
& -\frac{\tau \partial u}{\rho \partial z} - \frac{1}{2} u \frac{\partial \tau}{\partial z} - \left( \frac{\rho_s - \rho_w}{\rho} \right) g \left( \epsilon \frac{\partial c}{\partial z} \right) \\
& + \frac{\partial \left( \frac{\tau}{\rho U_1} \frac{\tau_{\max} Z}{\rho \delta} \right)}{\partial z} + \left[ \frac{\left( \frac{\tau}{\rho} \right)^{3/2}}{z} \right] \\
& = -\frac{R}{W} \left[ \frac{\partial \left[ \frac{\tau}{\rho U_1} \frac{\tau_{\max} Z}{\rho \delta} \right]}{\partial y} - u \frac{\partial \tau}{\partial y} \right] \\
& - \frac{R}{L} \left[ \frac{\partial \left[ \frac{\tau}{\rho U_1} \frac{\tau_{\max} Z}{\rho \delta} \right]}{\partial x} + u \frac{\partial \tau}{\partial x} \right. \\
& \quad \left. + w \frac{\partial \tau}{\partial z} - u \frac{\partial \tau}{\partial x} + w \frac{\partial \tau}{\partial z} + \frac{\tau \partial u}{\rho \partial x} + \frac{\tau \partial w}{\rho \partial z} \right] \\
& - \left( \frac{\Delta \rho}{\rho} g \frac{R}{\mathbb{U}^2} \right) \epsilon_{\max} \left( \frac{R}{L} \right)^2 \\
& \cdot \left[ \frac{\rho_s - \rho_w}{\rho} g \cos \theta \int \left[ \frac{\partial \left( \epsilon \frac{\partial c}{\partial x} \right)}{\partial x} \right] dz \right] \\
& + \frac{\nu_w}{\mathbb{U}R} \left[ \nu_w \frac{\partial^2 \tau}{\partial z^2} + \frac{\mu_w}{\rho} \frac{\partial}{\partial z} \left[ c \frac{\partial \left( \frac{\tau}{\rho} \right)}{\partial z} \right] (\partial z) \right] \\
& + \frac{R R}{L W} \left[ w \frac{\partial \left( \frac{\tau}{\rho} \right)}{\partial y} \right] \\
& - \left[ \frac{\Delta \rho}{\rho} g \frac{R}{\mathbb{U}^2} \right] \left( \frac{\epsilon_{\max}}{\mathbb{U}R} \right) \frac{R}{L} \sin \theta \left\{ \left[ \frac{\rho_s - \rho_w}{\rho} \right] g \left( \epsilon \frac{\partial c}{\partial x} \right) \right\} \\
& + \left( \frac{R}{L} \right)^2 \frac{\tau \partial w}{\rho \partial x} + \left( \frac{R}{W} \right)^2 \frac{\nu_w}{\mathbb{U}R} \left[ \frac{\mu_w}{\rho} \frac{\partial^2 \tau}{\partial y^2} + \frac{\mu_w}{\rho} c \frac{\partial^2 \tau}{\partial y^2} \right]
\end{aligned}$$

The term  $[(\tau/\rho)^{3/2}/z]$  in the left hand side of equation 31 does not present a singularity at  $(z = 0)$  since  $\lim_{z \rightarrow 0} [(\tau/\rho)^{3/2}/z] = 0$ .

Nine  $\pi$ -terms appear in eqs. 27–31 namely; the aspect ratios  $(R/L)$  and  $(R/W)$ ; the density gradient  $(\Delta\rho/\rho)$ ; a form of Ekman number  $E = (\epsilon_{\max}/fL^2)$ ; Reynolds number  $R = (\mathbb{U}R/\nu_w)$ ; a form of Richardson number  $R_* = (\mathbb{U}^2/(\Delta\rho/\rho)gR)$ ; which is Froudes number square  $(\mathbb{U}^2/gR)$  divided by the density gradient  $(\Delta\rho/\rho)$ ; Rossby number  $R_{**} = (\mathbb{U}/fL)$ ; and two forms of an eddy Reynolds number namely;  $R^* = (\rho \mathbb{U}^2/\tau_{\max})$  and  $R^{**} = (\mathbb{U}R/\epsilon_{\max})$ . The numerical values of the nine  $\pi$ -terms are as follows:  $(R/L) = 4.458 \times 10^{-5}$ ,  $(R/W) = 4.38 \times 10^{-3}$ ,  $(\Delta\rho/\rho) = 0.1416$ ,  $E = 1.05 \times 10^{-7}$ ,  $R = 1.6568 \times 10^5$ ,  $R_* = 1.0414 \times 10^{-4}$ ,  $R_{**} = 2.121 \times 10^{-3}$ ,  $R^* = 1.445$ , and  $R^{**} = 0.8968$ . The magnitude of each term in eqs. 27–31 is evaluated and the  $\pi$ -terms  $(R/L)$ ,  $(R/W)$ ,  $E$ ,  $R^{-1}$ ,  $R_*$ , and  $R_{**}$  are used as perturbation parameters. Perturbation methods for treating boundary layer problems (NAYFEH, 1985) are not used here; the equations of the zeroth approximation for the entire flow domain are solved analytically.

## THE ZEROTH APPROXIMATION

The equations of the zeroth approximation, eqs. 33–37 are obtained by setting the perturbation parameters equal to zero in eqs. 27–31 (VAN DYKE, 1964). To these equations, the equation of conservation of volume (eq. 8) is added in the form of eq. 32. Thus:

Equation of conservation of volume:

$$\frac{\partial u_0}{\partial x} + \frac{\partial w_0}{\partial z} = 0 \quad (32)$$

Equation of conservation of mass:

$$\frac{\partial \left( \epsilon_0 \frac{\partial c_0}{\partial z} \right)}{\partial z} + \frac{\rho_s}{\rho_s - \rho_w} \dot{w} \frac{\partial c_0}{\partial z} = 0 \quad (33)$$

Equation of conservation of momentum in the x-direction:

$$-\rho_s \dot{w} \frac{\partial (c_0 u_0)}{\partial z} + (\rho_s - \rho_w) g \cos \theta \int \frac{\partial c_0}{\partial x} dz - \frac{\partial \tau_0}{\partial z} = 0 \quad (34)$$

Equation of conservation of momentum in the y-direction:

$$[\rho_w + (\rho_s - \rho_w) c_0] f u_0 - \frac{\partial \tau_0}{\partial y} - \frac{\partial \tau_0}{\partial z} = 0 \quad (35)$$

Equation of conservation of momentum in the z-direction:

$$\rho_s \dot{w}^2 \frac{\partial c_0}{\partial z} + (\rho_s - \rho_w) g c + \frac{\partial \tau_0}{\partial z} = 0 \quad (36)$$

Equation of kinetic energy of turbulence:

$$\begin{aligned}
 & -u_0 \frac{\partial \left( \frac{\tau_0}{\rho_0} \right)}{\partial z} - \frac{\tau_0}{\rho_0} \frac{\partial u_0}{\partial z} - \frac{\rho_s - \rho_w}{\rho_0} g \left( \epsilon_0 \frac{\partial c_0}{\partial z} \right) \\
 & + \frac{\partial \left( \frac{\tau_0}{\rho_0 U_1 \rho_0 \delta} \right)}{\partial z} + \frac{\left( \frac{\tau_0}{\rho_0} \right)^{3/2}}{z} = 0 \quad (37)
 \end{aligned}$$

In eq. 37  $\tau_{\max}$  has been replaced by  $\tau$  in view of the absence of a reasonable estimate for  $\tau_{\max}$  and since  $\tau_{\max}$  has a significant effect on bed load movement rather than on suspended sediment which is the subject of the present study. In eqs. 32-37,  $\rho_0 \equiv [\rho_w + (\rho_s - \rho_w) c_0]$ ,  $\dot{w} = -1$ ,  $f = U_1 = \delta = 1$ , each of the coefficients  $[\rho_s/(\rho_s - \rho_w)]$ ,  $\rho_s$ ,  $(\rho_s - \rho_w)g \cos \theta$ ,  $\rho_w$ ,  $(\rho_s - \rho_w)$ , and  $(\rho_s - \rho_w)g$  is equal to one, and the subscript (o) refers to the zeroth approximation.

Substituting in eqs. 32-37 the numerical values of the constants and the coefficients and dropping the subscript (o) for convenience, the equations of the zeroth approximation take the form:

Equation of conservation of volume:

$$\frac{\partial u}{\partial x} + \frac{\partial w}{\partial z} = 0 \quad (38)$$

Equation of conservation of mass:

$$\frac{\partial \left( \epsilon \frac{\partial c}{\partial z} \right)}{\partial z} - \frac{\partial c}{\partial z} = 0 \quad (39)$$

Equation of conservation of momentum in the x-direction:

$$\frac{\partial(cu)}{\partial z} + \int \frac{\partial c}{\partial x} dz - \frac{\partial \tau}{\partial z} = 0 \quad (40)$$

Equation of conservation of momentum in the y-direction:

$$(1 + c)u - \frac{\partial \tau}{\partial y} - \frac{\partial \tau}{\partial z} = 0 \quad (41)$$

Equation of conservation of momentum in the z-direction:

$$\frac{\partial c}{\partial z} + c + \frac{\partial \tau}{\partial z} = 0 \quad (42)$$

Equation of kinetic energy of turbulence:

$$\begin{aligned}
 & -u \frac{\partial \left( \frac{\tau}{\rho} \right)}{\partial z} - \frac{\tau}{\rho} \frac{\partial u}{\partial z} - \epsilon \frac{\partial c}{\partial z} + \frac{\partial \left[ \left( \frac{\tau}{\rho} \right)^2 z \right]}{\partial z} + \frac{\left( \frac{\tau}{\rho} \right)^{3/2}}{z} = 0 \quad (43)
 \end{aligned}$$

## CONSTRUCTION OF THE SOLUTION OF THE ZEROth APPROXIMATION

### Solution for the Concentration of Suspended Sediment

Adding eqs. 40 and 42 then differentiating the resulting equation once with respect to  $z$  using Leibniz theorem for the differentiation of an integral results in:

$$(1 + u) \frac{\partial^2 c}{\partial z^2} + (1 + 2 \frac{\partial u}{\partial z}) \frac{\partial c}{\partial z}$$

$$+ (\partial^2 u / \partial z^2) c + \partial c / \partial x = 0 \quad (44)$$

The strategy is to reduce eq. 44 to a partial differential equation in the dependent variable  $c$ . To this end the velocity  $u$  is considered to be a function of  $z$  only; i.e.  $u = u(z)$ , and a logarithmic velocity profile is assumed. The assumption that  $u = u(z)$  is a reasonable one since the problem is formulated for flow near slack where the changes in  $u$  in the  $x$ -direction are small compared with the changes in the  $z$ -direction. This assumption simplifies the solution of eq. 44 for  $c$ . The concentration of suspended sediment  $c$  is obtained from the solution of the boundary value problem given by eq. 45.

$$\begin{aligned}
 & (1 + u) \frac{\partial^2 c}{\partial z^2} + \left( 1 + 2 \frac{\partial u}{\partial z} \right) \frac{\partial c}{\partial z} + \frac{d^2 u}{dz^2} c + \frac{\partial c}{\partial x} = 0; \\
 & c(0, 0) \equiv (c_0) = 1, \quad c(x, 1) = 0, \quad c(0, z) = f(z) \quad (45)
 \end{aligned}$$

where  $f(z)$  is a given function. A separable solution is selected in the form:

$$c(x, z) = X(x)Z(z) \quad (46)$$

Substituting equation 46 into equation 45 and dividing by  $X(x)Z(z)$  results in:

$$(1 + u) \frac{Z''}{Z} + \left( 1 + 2 \frac{du}{dz} \right) \frac{Z'}{Z} + \frac{d^2 u}{dz^2} = -\frac{X'}{X} \quad (47)$$

Taking the partial derivatives with respect to  $x$  of both sides of the separated equation 47, it is found that:

$$\frac{d \left[ \frac{X'}{X} \right]}{dx} = 0,$$

which by integration becomes:

$$X' - \beta X = 0 \quad (48)$$

where  $\beta$  is a separation constant. Then

$$(1 + u) \frac{Z''}{Z} + \left( 1 + 2 \frac{du}{dz} \right) \frac{Z'}{Z} + \frac{d^2 u}{dz^2} = -\beta \quad (49)$$

Equation 49 is written in the form:

$$Z'' + \sigma(z)Z' + \omega(z)Z = 0 \quad (50)$$

where

$$\sigma(z) = \frac{1 + 2 \frac{du}{dz}}{1 + u},$$

and

$$\omega(z) = \frac{\frac{d^2 u}{dz^2} + \beta}{1 + u}$$

Thus,  $c(x, z) = X(x)Z(z)$  is the solution of equation 45 if and only if  $X$  and  $Z$  satisfy the two ordinary differential equations 48 and 50 for the specified boundary conditions for some  $\beta$ .  $X(x)$  and  $Z(z)$  respectively, are the solutions of the boundary value problems given by equations 51 and 52.

$$X' - \beta X = 0; \quad X(0) = 1 \quad (51)$$

$$Z'' + \sigma(z)Z' + \omega(z)Z = 0; \quad Z(0) = 1, \quad Z(1) = 0 \quad (52)$$

The solution of the boundary value problem given by equation 51 is:

$$X = e^{\beta x} \quad (53)$$

The solution of the boundary value problem given by equation 52 is obtained by substituting, in equation 52, the three consecutive transformations given by equations 54–56 (KAMKE, 1971), resulting in equation 57.

$$v(z) = \frac{Z'}{Z} \quad (54)$$

$$\varphi(z) = v(z) + \frac{1}{2}\sigma(z) \quad (55)$$

$$\varphi(z) = \frac{\Phi'(z)}{\Phi(z)} \quad (56)$$

$$\Phi'' + \psi(z)\Phi = 0; \quad \Phi(0) = 1, \quad \Phi(1) = 0 \quad (57)$$

where

$$\psi(z) = -\frac{\sigma}{2} - \frac{\sigma^2}{4} + \omega.$$

The transformation from  $Z(z)$  to  $\Phi(z)$  is affected by equation 58.

$$Z = e^{(-z/4)}\Phi \quad (58)$$

The boundary value problem given by eq. 57 could be formulated as a Fredholm integral equation with degenerate kernel and solved by reducing it to a system of linear algebraic equations (KAMEL, 1978). The boundary value problem could be also formulated as an integral equation with symmetric kernel where Green's function is represented in terms of the Fourier series of the orthonormal eigenfunctions,  $(2)^{1/2} \sin(n\pi z)$ ,  $n = 1, 2, \dots$ , (CHAMBRE, 1977). As a change of pace, the solution of the boundary value problem given by eq. 57 would be presented as a Fourier series of the eigenfunctions of the Sturm-Liouville problem given by eq. 59.

$$\xi'' + \lambda_n \xi = 0; \quad \xi(0) = 0, \quad \xi(1) = 0 \quad (59)$$

A considerable reduction in the mathematical labor could be achieved, without much sacrifice in the accuracy of the solution, by replacing  $\psi(z)$  by a constant. This is possible by setting  $u = 1$  in the expression for  $\psi(z)$ . The assumption that  $u = 1$ , a constant, is based on the uniformity of the logarithmic velocity profile except near the bed. The assumption does not significantly affect the partial differential equation since it only affects the coefficients which become numbers instead of functions of  $z$ . Affecting this assumption, the boundary value problem given by eqs. 45 and 57 respectively reduce to eqs. 60 and 61.

$$\frac{\partial^2 c}{\partial z^2} + \frac{1}{2} \frac{\partial c}{\partial z} + \frac{1}{2} \frac{\partial c}{\partial x} = 0,$$

$$c(0, 0) (\equiv c_0) = 1, \quad c(x, 1) = 0; \quad c(0, z) = f(z). \quad (60)$$

$$\Phi'' + \gamma \Phi = 0; \quad \Phi(0) = 1, \quad \Phi(1) = 0 \quad (61)$$

where  $\gamma = (\beta/2 - 1/16)$ . To reduce the boundary value problem given by equation 61 to one with homogeneous end conditions, substitute for  $\Phi$  a function  $\zeta = (1 - z)$  which satisfies these boundary conditions. Then the difference  $\eta = \Phi - \zeta$  satisfies a nonhomogeneous equation with homogeneous end conditions, *i.e.*,

$$\eta = \Phi - (1 - z) \quad (62)$$

Substituting equation 62 into equation 61, the latter takes the form:

$$\eta'' + \gamma[\eta + (1 - z)] = 0,$$

*i.e.*

$$-\eta'' = \gamma\eta + \Delta(z), \quad \Delta(z) = \gamma(1 - z) \quad (63)$$

The Sturm-Liouville problem given by equation 59 has the eigenvalues ( $\lambda_n$ ) and eigenfunctions ( $\phi_n$ ) given by:

$$\lambda_n = (n\pi)^2, \quad n = 1, 2, \dots; \quad \phi_n(z) = 2^{1/2} \sin(\lambda_n^{1/2} z) \quad (64)$$

The solution of equation 63 in terms of the eigenfunctions ( $\phi_n$ ) is given by the Fourier sine series, equation 65 (Myint-U, 1987).

$$\eta = \sum_{n=1}^{\infty} b_n \phi_n(z),$$

where

$$b_n = \frac{C_n}{\lambda_n - \gamma},$$

$$C_n = \int_0^1 [\gamma(1 - z)\phi_n^{1/2}] dz = \left(\frac{2}{\lambda_n}\right)^{1/2} \gamma \quad (65)$$

*i.e.*,

$$\eta = 2\gamma \sum_{n=1}^{\infty} \frac{\sin(\lambda_n^{1/2} z)}{\lambda_n^{1/2}(\lambda_n - \gamma)}$$

By equation 65 in equation 62, it follows that:

$$\Phi = 2\gamma \sum_{n=1}^{\infty} \frac{\sin(\lambda_n^{1/2} z)}{\lambda_n^{1/2}(\lambda_n - \gamma)} + (1 - z) \quad (66)$$

Affecting the transformation given by equation 58, equation 66 takes the form:

$$Z(z) = e^{(-z/4)} \left[ 2\gamma \sum_{n=1}^{\infty} \frac{\sin(\lambda_n^{1/2} z)}{\lambda_n^{1/2}(\lambda_n - \gamma)} + (1 - z) \right] \quad (67)$$

By equations 67 and 53 in equation 46, it follows that:

$$c(x, z) = e^{(\beta x - z/4)} \left[ 2\gamma \sum_{n=1}^{\infty} \frac{\sin(\lambda_n^{1/2} z)}{\lambda_n^{1/2}(\lambda_n - \gamma)} + (1 - z) \right] \quad (68)$$

where  $\gamma = [(\beta/2) - (1/16)]$  and  $\lambda_n = (n\pi)^2$ ,  $n = 1, 2, \dots$

After expanding  $(1 - z)$  in terms of the eigenfunction  $\phi_n$ , it is easy, as given later in this section, to verify that eq. 68 is the solution of the boundary value problem given by eq. 60 except for not satisfying the boundary condition  $c(0, z) = f(z)$ . To this end set  $x = 0$  in eq. 68, the latter takes the form:

$$c(0, z) = f(z) = e^{z/4} \left[ 2\gamma \sum_{n=1}^{\infty} \frac{\sin(\lambda_n^{1/2} z)}{\lambda_n^{1/2}(\lambda_n - \gamma)} + (1 - z) \right] \quad (69)$$

i.e.,

$$f(z) e^{z/4} - (1 - z) = 2\gamma \sum_{n=1}^{\infty} \frac{\sin(\lambda_n^{1/2} z)}{\lambda_n^{1/2}(\lambda_n - \gamma)},$$

written as:

$$\begin{aligned} f(z)e^{z/4} - (1 - z) &= \sum_{n=1}^{\infty} \frac{2\gamma \sin(\lambda_n^{1/2} z)}{\lambda_n^{1/2}(\lambda_n - \gamma)} \\ &= \sum_{n=1}^{\infty} \frac{2\gamma}{\lambda_n^{1/2}(\lambda_n - \gamma)} \sin(\lambda_n^{1/2} z) \end{aligned} \quad (70)$$

provided that  $[f(z)e^{z/4} - (1 - z)]$  is a piecewise smooth function defined on  $0 < z < 1$ , its Fourier sine series is:

$$\begin{aligned} &\sum_{n=1}^{\infty} \alpha_n \sin(\lambda_n^{1/2} z), \\ \alpha_n &= 2 \int_0^1 [f(z)e^{z/4} - (1 - z)] \sin(\lambda_n^{1/2} z) dz \end{aligned} \quad (71)$$

i.e.,

$$\begin{aligned} \alpha_n &= 2 \int_0^1 f(z)e^{z/4} \sin(\lambda_n^{1/2} z) dz \\ &\quad - 2 \int_0^1 (1 - z) \sin(\lambda_n^{1/2} z) dz \\ &= a_n - \frac{2}{\lambda_n^{1/2}}, \\ a_n &= 2 \int_0^1 f(z)e^{z/4} \sin(\lambda_n^{1/2} z) dz \end{aligned} \quad (72)$$

Equating equations 70 and 71 results in equation 73.

$$\begin{aligned} &\sum_{n=1}^{\infty} \frac{2\gamma}{\lambda_n^{1/2}(\lambda_n - \gamma)} \sin(\lambda_n^{1/2} z) \\ &= \sum_{n=1}^{\infty} \left\{ 2 \int_0^1 [f(z) e^{z/4} - (1 - z)] \sin(\lambda_n^{1/2} z) dz \right. \\ &\quad \left. \cdot [\sin(\lambda_n^{1/2} z)] \right\} \end{aligned} \quad (73)$$

It follows that the boundary condition  $c(0, z) = f(z)$  is satisfied if:

$$\frac{2\gamma}{\lambda_n^{1/2}(\lambda_n - \gamma)} = 2 \int_0^1 [f(z)e^{z/4} - (1 - z)] \sin(\lambda_n^{1/2} z) dz \quad (74)$$

By equation 74 in equation 68, it follows that:

$$\begin{aligned} c(x, z) &= e^{(\beta x - z/4)} \left\{ \sum_{n=1}^{\infty} \left[ 2 \int_0^1 [f(z)e^{z/4} - (1 - z)] \sin(\lambda_n^{1/2} z) dz \right. \right. \\ &\quad \left. \left. \cdot [\sin(\lambda_n^{1/2} z)] \right] + (1 - z) \right\} \end{aligned} \quad (75)$$

The verification that equation 75 is the solution of the boundary value problem given by equation 60 is as follows: By inspection of equation 75 it is seen that  $c(0, 0) = 1$  and  $c(x, 1) = 0$ . To verify the boundary condition  $c(0, z) = f(z)$ , set  $x = 0$  in equation 75, the latter takes the form:

$$\begin{aligned} c(0, z) &= e^{(-z/4)} \left\{ \sum_{n=1}^{\infty} \left[ 2 \int_0^1 [f(z)e^{z/4} - (1 - z)] \sin(\lambda_n^{1/2} z) dz \right. \right. \\ &\quad \left. \left. \cdot [\sin(\lambda_n^{1/2} z)] \right] + (1 - z) \right\} \end{aligned} \quad (76)$$

By equation 73 in equation 76, the latter takes on the form:

$$c(0, z) = e^{(-z/4)} \left\{ \sum_{n=1}^{\infty} \left[ \left( \frac{2\gamma}{\lambda_n^{1/2}(\lambda_n - \gamma)} \right) \sin(\lambda_n^{1/2} z) \right] + (1 - z) \right\} \quad (77)$$

$\equiv f(z)$  by equation 69, thus verifying the boundary condition  $c(0, z) = f(z)$ . To verify that eq. 75 is the solution of the partial differential equation 60, set

$$2 \int_0^1 [f(z)e^{z/4} - (1 - z)] \sin(\lambda_n^{1/2} z) dz \equiv \alpha_n = a_n - \frac{2}{\lambda_n^{1/2}},$$

equation 75 takes the form:

$$c(x, z) = e^{(\beta x - z/4)} \left( \sum_{n=1}^{\infty} \left\{ \left[ a_n - \left( \frac{2}{\lambda_n^{1/2}} \right) \right] \sin(\lambda_n^{1/2} z) \right\} + (1 - z) \right) \quad (78)$$

Differentiation of equation 78 results in

$$\frac{\partial c}{\partial x} = \beta e^{(\beta x - z/4)} \left( \sum_{n=1}^{\infty} \left\{ \left[ a_n - \frac{2}{\lambda_n^{1/2}} \right] \sin(\lambda_n^{1/2} z) \right\} + (1 - z) \right) \quad (79)$$

$$\begin{aligned} \frac{\partial c}{\partial z} &= -\frac{1}{4} e^{(\beta x - z/4)} \left( \sum_{n=1}^{\infty} \left\{ \left[ a_n - \left( \frac{2}{\lambda_n^{1/2}} \right) \right] \sin(\lambda_n^{1/2} z) \right\} + (1 - z) \right) \\ &\quad + e^{(\beta x - z/4)} \left( \sum_{n=1}^{\infty} \left\{ \left[ a_n - \frac{2}{\lambda_n^{1/2}} \right] (\lambda_n^{1/2}) \cos(\lambda_n^{1/2} z) \right\} - 1 \right) \end{aligned} \quad (80)$$

$$\begin{aligned} \frac{\partial^2 c}{\partial z^2} &= \frac{1}{16} e^{(\beta x - z/4)} \left( \sum_{n=1}^{\infty} \left\{ \left[ a_n - \frac{2}{\lambda_n^{1/2}} \right] \sin(\lambda_n^{1/2} z) \right\} + (1 - z) \right) \\ &\quad - \frac{1}{2} e^{(\beta x - z/4)} \left( \sum_{n=1}^{\infty} \left\{ \left[ a_n - \frac{2}{\lambda_n^{1/2}} \right] \lambda_n^{1/2} \cos(\lambda_n^{1/2} z) \right\} - 1 \right) \\ &\quad + e^{(\beta x - z/4)} \left( \sum_{n=1}^{\infty} \left\{ (-) \left[ a_n - \left( \frac{2}{\lambda_n^{1/2}} \right) \right] \lambda_n \sin(\lambda_n^{1/2} z) \right\} \right) \end{aligned} \quad (81)$$

Substituting for

$$(1 - z) = 2 \sum_{n=1}^{\infty} \frac{1}{\lambda_n^{1/2}} \sin(\lambda_n^{1/2} z)$$

in equations 79–81, it follows that:

$$\begin{aligned} & \frac{\partial^2 c}{\partial z^2} + \frac{1}{2} \frac{\partial c}{\partial z} + \frac{1}{2} \frac{\partial c}{\partial x} \\ & = e^{(\beta x - z/4)} \sum_{n=1}^{\infty} \left( \left[ \frac{1}{16} a_n - \frac{2}{\lambda_n^{1/2}} + \frac{2}{\lambda_n^{1/2}} \right] \right. \\ & \quad \left. - \lambda_n \left( a_n - \frac{2}{\lambda_n^{1/2}} \right) - \frac{1}{8} \left[ a_n - \frac{2}{\lambda_n^{1/2}} + \frac{2}{\lambda_n^{1/2}} \right] \right. \\ & \quad \left. + \frac{\beta}{2} \left[ a_n - \frac{2}{\lambda_n^{1/2}} + \frac{2}{\lambda_n^{1/2}} \right] \sin(\lambda_n^{1/2} z) \right) \\ & = e^{(\beta x - z/4)} \sum_{n=1}^{\infty} \left( \left[ \frac{a_n}{16} - \lambda_n \left[ a_n - \frac{2}{\lambda_n^{1/2}} \right] \right. \right. \\ & \quad \left. \left. - \frac{a_n}{8} + \frac{\beta}{2} a_n \right] \sin(\lambda_n^{1/2} z) \right) = 0 \end{aligned}$$

if and only if

$$\left\{ \frac{a_n}{16} - \lambda_n a_n + 2\lambda_n^{1/2} - \frac{a_n}{8} + \frac{a_n \beta}{2} \right\} = 0.$$

i.e.,

$$\beta = 2\lambda_n - \frac{4\lambda_n^{1/2}}{a_n} + \frac{1}{8} \quad (82)$$

Therefore eq. 75 is the solution of the boundary value problem given by eq. 60 if and only if eq. 82 is satisfied. By eq. 82 in eq. 75, it follows that the solution of the boundary value problem given by eq. 60 is:

$$\begin{aligned} c(x, z) = e^{(\beta x - z/4)} & \left\{ \sum_{n=1}^{\infty} \left[ \left( 2 \int_0^1 \{ [f(z)e^{z/4} - (1-z)] \sin \lambda_n^{1/2} z \} dz \right) \right. \right. \\ & \left. \left. \cdot [\sin(\lambda_n^{1/2} z)] \right] + (1-z) \right\} \end{aligned} \quad (83)$$

where:

$$\lambda_n = (n\pi)^2,$$

$$n = 1, 2, \dots;$$

$$\beta = \left( 2\lambda_n - \frac{4\lambda_n^{1/2}}{a_n} + \frac{1}{8} \right);$$

$$a_n = 2 \int_0^1 [f(z)e^{z/4} \sin(\lambda_n^{1/2} z)] dz,$$

a number.

### Solution for the Coefficient of Exchange of Mass

The coefficient of exchange of mass  $\epsilon(x, z)$  is obtained from the solution of the boundary value problem given by eq. 84.

$$\partial(\epsilon \partial c / \partial z) / \partial z - \partial c / \partial z = 0; \quad \epsilon(x, 0) = 0 \quad (84)$$

Integration of eq. 84 once with respect to  $z$ , results in eq. 85.

$$(\epsilon \partial c / \partial z) - c = f(x) \quad (85)$$

Imposing in eq. 85 the boundary condition  $\epsilon(x, 0) = 0$ , it fol-

lows that  $f(x) = -c(x, 0)$  which when substituted in eq. 85, results in:

$$\epsilon = [c(x, z) - c(x, 0)] / (\partial c / \partial z) \quad (86)$$

By eq. 80 in eq. 86, the solution for the coefficient of exchange of mass is obtained as:

$$\begin{aligned} \epsilon(x, z) & = \left( e^{(\beta x - z/4)} \left\{ \sum_{n=1}^{\infty} \left[ \left( a_n - \frac{2}{\lambda_n^{1/2}} \right) \sin(\lambda_n^{1/2} z) \right] + (1-z) \right\} - e^{\beta x} \right) \\ & \quad \cdot \left( -\frac{1}{4} e^{(\beta x - z/4)} \left\{ \sum_{n=1}^{\infty} \left[ \left( a_n - \frac{2}{\lambda_n^{1/2}} \right) \sin(\lambda_n^{1/2} z) \right] + (1-z) \right\} \right. \\ & \quad \left. + e^{(\beta x - z/4)} \left\{ \sum_{n=1}^{\infty} \left[ \left( a_n - \frac{2}{\lambda_n^{1/2}} \right) \lambda_n^{1/2} \cos(\lambda_n^{1/2} z) \right] - 1 \right\} \right)^{-1} \end{aligned} \quad (87)$$

### Solution for the Turbulent Shear Stress

The solution for the turbulent shear stress  $\tau(x, z)$  is obtained from the solution of the boundary value problem given by eq. 42 subject to the boundary condition  $\tau(x, 0) = 0$ , i.e.

$$\partial c / \partial z + c + \partial \tau / \partial z = 0; \quad \tau(x, 0) = 0 \quad (88)$$

Rearranging the partial differential equation as  $\partial \tau / \partial z = -c - \partial c / \partial z$  and integrating once with respect to  $(z)$ , results in eq. 89.

$$\tau = -\int c dz - c + g(x) \quad (89)$$

Imposing in equation 89 the boundary condition  $\tau(x, 0) = 0$ , results in:

$$0 = -\int c(x, z) dz \Big|_{z=0} - c(x, 0) + g(x);$$

i.e.,

$$g(x) = c(x, 0) + \int c(x, z) dz \Big|_{z=0} \quad (90)$$

By equation 90 in equation 89, the solution for the turbulent shear stress is given as:

$$\tau(x, z) = -\int c(x, z) dz - c(x, z) + c(x, 0) + \int c(x, z) dz \Big|_{z=0} \quad (91)$$

The solution for the turbulent shear stress  $\tau(x, y, z)$  is obtained from the solution of the boundary value problem given by equation 41 subject to the boundary condition given by equation 91. i.e.,

$$(1 + c)u - \frac{\partial \tau}{\partial y} - \frac{\partial \tau}{\partial z} = 0;$$

$$\tau(x, z) = -\int c(x, z) dz - c(x, z) + c(x, 0) + \int c(x, z) dz \Big|_{z=0} \quad (92)$$

Integrating eq. 41 once with respect to  $z$  and imposing the boundary condition given by eq. 91 results in the solution of the boundary value problem given by eq. 92 as:

$$\tau(x, y, z) = \tau(x, z) + \{[\partial\tau(x, z)/\partial z] - (1 + c)u\}y \quad (93)$$

where  $\tau(x, z)$  is given by eq. 91,  $c(x, z)$  is given by eq. 83, and a logarithmic velocity profile is assumed, for the longitudinal velocity of the flow, in the form:

$$u \cong 1 + 0.1848 \ln(z + 0.004465) \quad (94)$$

**Solution for the Longitudinal Velocity of the Flow**

The longitudinal velocity of the flow  $u$  is obtained from the solution of the boundary value problem given by eq. 43 subject to the boundary condition  $u(x, 0) = 0$ , i.e.

$$-u\partial(\tau/\rho)/\partial z - (\tau/\rho)\partial u/\partial z - (\epsilon\partial c/\partial z) + \partial[(\tau/\rho)^2 z]/\partial z + (\tau/\rho)^{3/2}/z = 0; u(x, 0) = 0 \quad (95)$$

The boundary value problem given by eq. 95 is written as:

$$\partial u/\partial z + h(x, z)u = k(x, z); u(x, 0) = 0 \quad (96)$$

where

$$h(x, z) = (1/2)[\partial(\tau/\rho)/\partial z]/(\tau/\rho), k(x, z) = -[\epsilon\partial c/\partial z] + [\partial(\tau/\rho)^2 z/\partial z] + [(\tau/\rho)^{3/2}/z] \quad (97)$$

The solution of the boundary value problem given by eq. 96 is:

$$u(x, z) = \exp \left\{ - \int \left[ \frac{1}{2} \frac{\partial \left( \frac{\tau}{\rho} \right)}{\partial z} \right] \left( \frac{\tau}{\rho} \right)^{-1} dz \right\} \cdot \int \left\{ - \epsilon \frac{\partial c}{\partial z} + \frac{\partial \left( \frac{\tau}{\rho} \right)^2 z}{\partial z} + \frac{\left( \frac{\tau}{\rho} \right)^{3/2}}{z} \right\} \cdot \exp \left\{ \int \left[ \frac{1}{2} \frac{\partial \left( \frac{\tau}{\rho} \right)}{\partial z} \right] \left( \frac{\tau}{\rho} \right)^{-1} dz \right\} dz \quad (98)$$

No attempt is made to solve eq. 38 for the vertical velocity  $w$  since the equations are getting to be cumbersome; a solution for  $w$  was given by KAMEL (1976) and shows that  $w$  is maximum at the water surface and decreases to zero at the bottom of the estuary. Eqs. 83, 87, 93, and 98 respectively give the solution of the zeroth approximation for the concentration of suspended sediment  $c$ , the coefficient of exchange of mass  $\epsilon$ , the turbulent shear stress  $\tau$ , and the longitudinal velocity of the flow  $u$ .

**RESULTS**

**The Concentration of Suspended Sediment**

The sediment concentration profiles which were used as  $f(z)$  in the boundary condition  $c(0, z) = f(z)$ , eq. 45, are shown

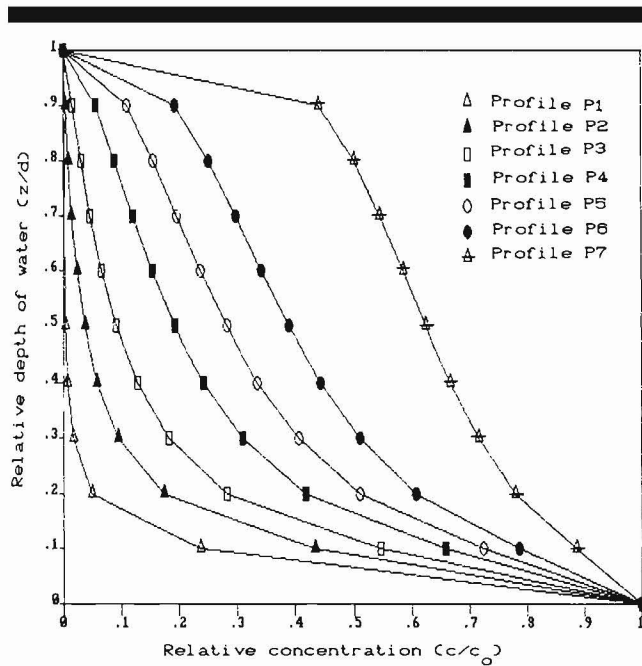


Figure 8. Sediment concentration profiles studied (ASCE, 1963).

in Figure 8 (ASCE, 1963). The figure shows a plot of the relative concentration ( $c/c_0$ ) versus the relative depth of water ( $z/d$ ). The data used in the figure is the result of measurements of the distribution of suspended sediment made by several researchers in natural streams and canals and in laboratory flumes. Mathematical necessity required that the data in Figure 8 be presented as: (i) ( $c/c_0$ ) on the  $x$ -axis instead of ( $c/c_a$ ) as originally given in ASCE (1963) where  $c_a$  is the concentration at a distance  $a$  from the bottom of the channel equal to 0.05 the water depth; (ii) the origin of the  $z$ -axis is at ( $z/d$ ) = 0 instead of ( $z/d$ ) =  $a$  as in ASCE (1963). Figure 9 shows the results obtained for the variation of the concentration of suspended sediment  $c$  with the relative depth of water ( $z/d$ ) and along the estuary for an assumed bottom concentration at the beginning of the estuary  $c_0 \equiv c(0, 0) = 1$ . Since  $\partial c/\partial x$  is positive, it follows that the concentration of suspended sediment increases along the estuary as shown in Figure 9; this is in agreement with previous research work on sedimentation.

To save journal space the results are presented for only one of the seven concentration profiles. In one instance, clarity of the presentation required presenting the results for two profiles.

**The Coefficient of Exchange of Mass**

Figure 10 shows the variation of the coefficient of exchange of mass  $\epsilon$  with the relative depth of water ( $z/d$ ) for profiles P1-P7 of Figure 8. It can be seen from the figure that  $\epsilon$  increases from zero at the bottom to a maximum value at about ( $z/d$ ) = 0.1 then decreases to a nearly constant value towards the water surface. This is in agreement with the profile of  $\epsilon$  reported by ICHIVE (1966) for the nepheloid layer on the At-

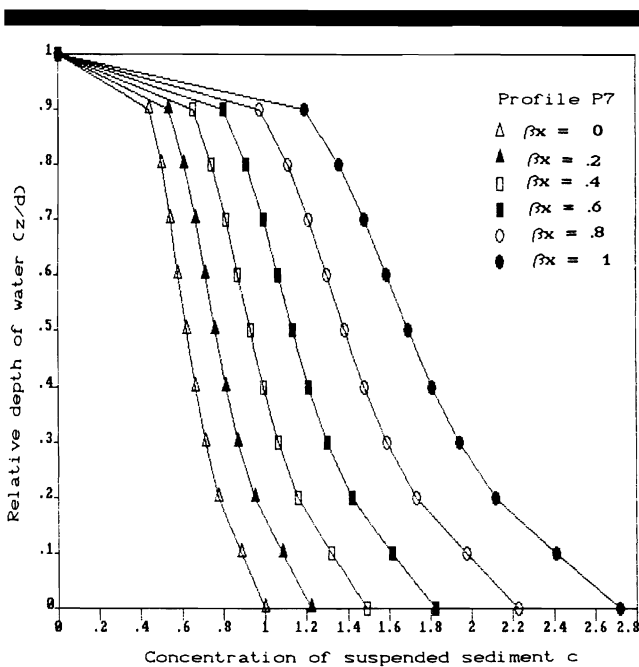


Figure 9. Variation of the concentration of suspended sediment along the estuary.

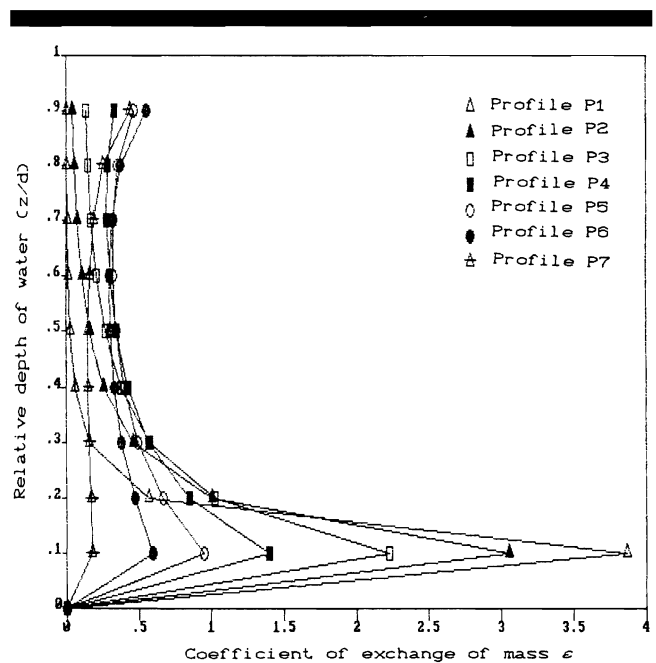


Figure 10. Variation of the coefficient of exchange of mass with the relative depth of water.

lantic slope, which was determined from measured vertical profiles of suspensoid. ICHIYE (1966) reported that  $\epsilon$  increase from zero at the bottom of the sea to a maximum value at 100 to 200 (m) then decreases and reaches some constant value towards the water surface.

The field data for the Enoree river originally reported by COLMAN (1969) and later reported by VAN RIJIN (1984), [Figure 5 page 1620], as a plot of  $(\epsilon/u_{*o}d)$  versus  $(z/d)$  is used for the verification of the results of  $\epsilon$  as shown in Figure 11. The figure shows a plot of  $(\epsilon/u_{*o}d)/(\epsilon/u_{*o}d)_{\max}$  versus  $(z/d)$  for profile P3 and for the data reported by VAN RIJIN (1984). The reason for the disagreement between the analytical results and the data reported by VAN RIJIN (1984) is that in the present study  $\epsilon$  is given by eq. 86 as  $\epsilon = [c(x, z) - c(x, 0)]/(\partial c/\partial z)$  which is the solution of the second order partial differential equation  $\partial(\epsilon \partial c/\partial z)/\partial z - (\partial c/\partial z) = 0$  [eq. 39]; while in VAN RIJIN (1984)  $\epsilon$  is computed from the measured concentration profiles using the first order differential equation  $\epsilon = -wc/(dc/dz)$ .

### The Turbulent Shear Stress

The expressions for the turbulent shear stress  $\tau$  and for the longitudinal velocity of the flow  $u$  given by eqs. 93 and 98 respectively, are too cumbersome for mathematical manipulation to find out the behaviour of the profiles of  $\tau$  and  $u$  and the effect of the concentration of suspended sediment on these profiles. Consequently in what follows the analysis would be based on the interpretation of the numerical results obtained from the solution of these two equations.

The results obtained for the turbulent shear stress  $\tau$  are shown in Figures 12–15. The results shown in Figures 12–14

are for  $\tau(x, 0, z)$  while the results shown in Figure 15 are for  $\tau(1, y, z)$ ; similar results are obtained for arbitrary values of  $y$  and of  $x$  respectively. Figures 12 and 13 show the variation of  $(\tau/\rho u^2)$  with the relative depth of water  $(z/d)$ ; the figures show that  $(\tau/\rho u^2)$  increases from zero at the bottom to a maximum value at a relative depth of about 0.2 then decreases towards the water surface. The figures also show the effect of the concentration of suspended sediment on the profile of the turbulent shear stress. Figure 12 shows that for the same bottom concentration  $c_o$ ,  $(\tau/\rho u^2)$  decreases with the increase in the uniformity of the concentration distribution, e.g.  $(\tau/\rho u^2)$  for profile P1 where the concentration distribution decays rapidly towards the water surface as shown in Figure 8, is larger than  $(\tau/\rho u^2)$  for profile P7 where the concentration distribution is more uniform. Figure 13 is a plot of  $(\tau/\rho u^2)$  versus  $(z/d)$ , for profile P5, for bottom concentrations  $c_o = 1, 1.2214, 1.4918, 1.8221, 2.2255, \text{ and } 2.7183$ . The figure shows that  $(\tau/\rho u^2)$  is nearly invariant for the different bottom concentrations. Figure 14, a plot of  $(\tau/\rho u^2)/(\tau/\rho u^2)_{\max}$  versus  $(z/d)$  for profile P4, exhibits the same trend shown in Figure 13. A study which has some bearing on the above findings is that of KARIM and KENNEDY (1987) who reported that for  $(\bar{w} > U S)$ , which is the case in the present study, the suspended sediment contributes less energy to the flow than its settling dissipates suggesting that an increase in the concentration would result in a decrease in the energy available to the flow.

The variation of the shear stress in the  $y$ -direction is shown in Figure 15. The figure shows a plot of  $(\tau/\rho u^2)$  versus  $(z/d)$ , for profile P3 of Figure 8 for  $y$  values of 0, [0.1], [0.2], [0.3], [0.4], and [0.5]; here  $y = 0$  denotes the center line of the estuary. It can be seen from the figure that  $(\tau/\rho u^2)$  increases away from the center line of the estuary towards its sides; at

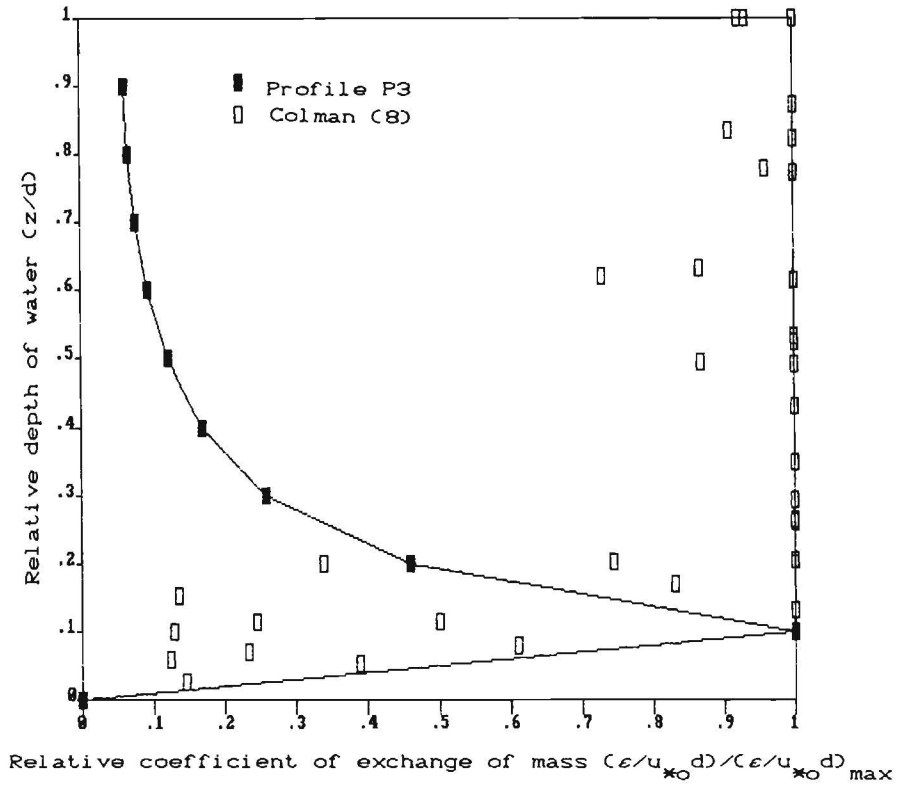


Figure 11. Verification of the relative coefficient of exchange of mass using the field data of Colman (1969), taken from van Rijn (1984).

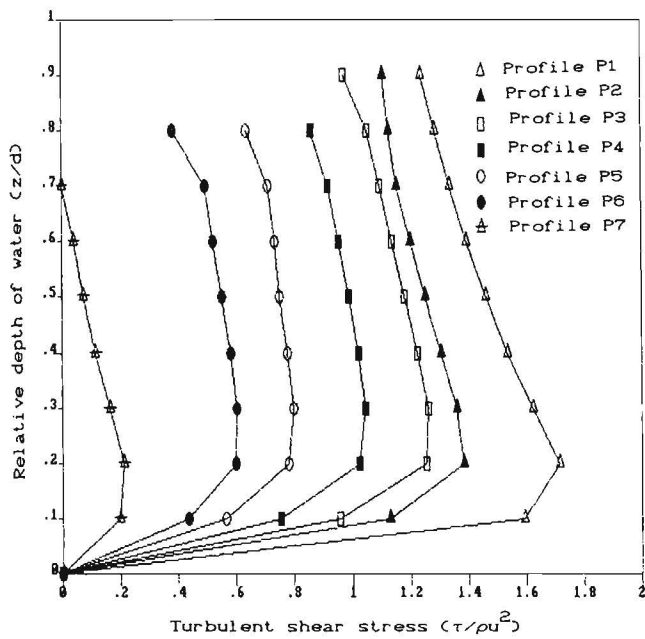


Figure 12. Variation of  $(\tau/\rho u^2)$  with the relative depth of water.

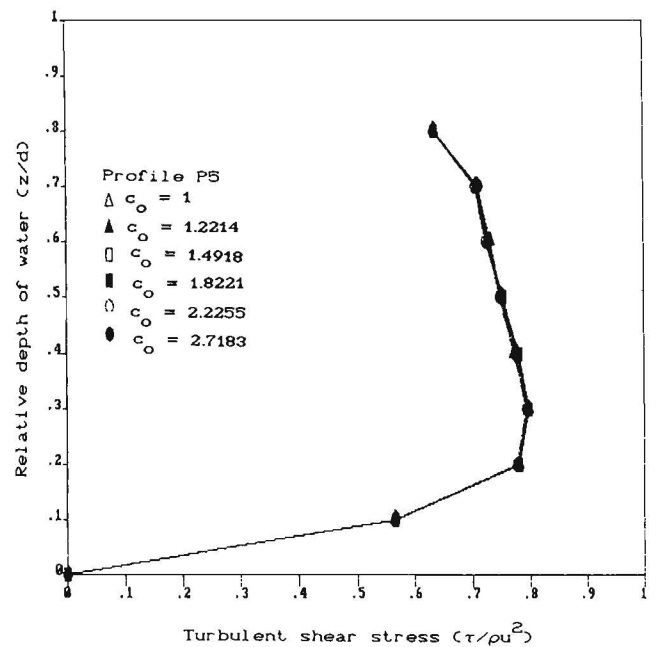


Figure 13. Effect of the concentration of suspended sediment on the profile of  $(\tau/\rho u^2)$ .

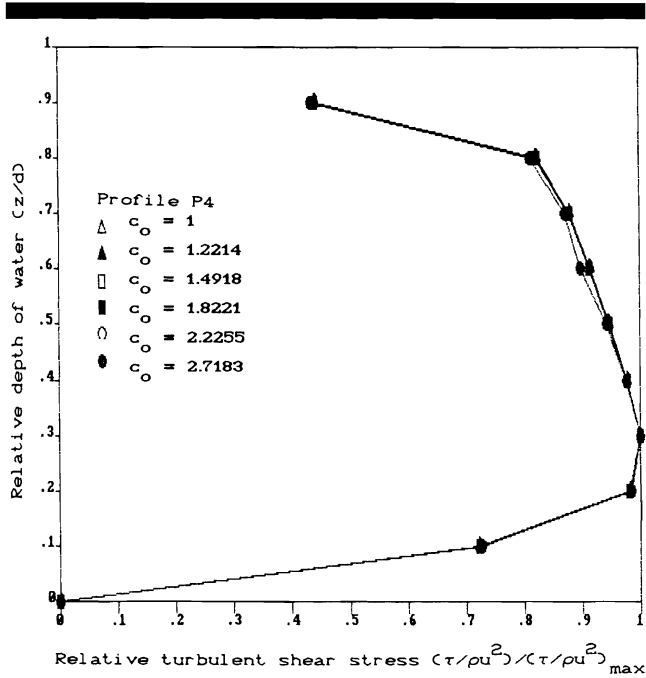


Figure 14. Effect of the concentration of suspended sediment on the profile of  $[(\tau/\rho u^2)/(\tau/\rho u^2)_{\max}]$ .

the sides the shear stress would be zero although this boundary condition was not affected in the solution since  $\tau(x, y, z)$  is obtained from the solution of the first order partial differential equation 92 which required imposing one boundary condition, namely  $\tau(x, 0, z) = \tau(x, z)$  as given by eq. 92. The literature does not appear to have experimental data on the three dimensional distribution of the turbulent shear stress. However, in a three dimensional analytical model of secondary flow, shear stress, and sediment transport for Rio Grande conveyance channel, CHIU and HSIUNG (1981) obtained a shear stress distribution in the y-direction (Figures 2, 5, and 7, respectively pp. 886, 889, and 890), similar to the one obtained from the present study and shown in Figure 15.

The experimental data available for the verification of the analytical findings of this study is scarce, even more scarce is the data which corresponds to conditions similar to the present study. The experimental data of ALFRINK and VAN RIJIN (1983), KOUTITAS and O'CONNOR (1981), and LYN (1988) is used for the verification. Of the above flume data that of LYN (1988) is the only data which corresponds to conditions similar to the present study in that the data is for turbulent open channel flow over a flat well sorted natural sand bed in equilibrium with a suspension of sand. The data of ALFRINK and VAN RIJIN (1983) is for flow in a steep-sided trench perpendicular to the main flow direction. The data of KOUTITAS and O'CONNOR (1981) is for a steep-sided channel, dredged at right angles to the main direction of the flow and sediment transport. In order to compare the results obtained from the present study with those of ALFRINK and VAN RIJIN (1983), KOUTITAS and O'CONNOR (1981), and LYN (1988), the results are presented as a plot of  $(\tau/\tau_{\max})$  versus  $(z/d)$ . Figure

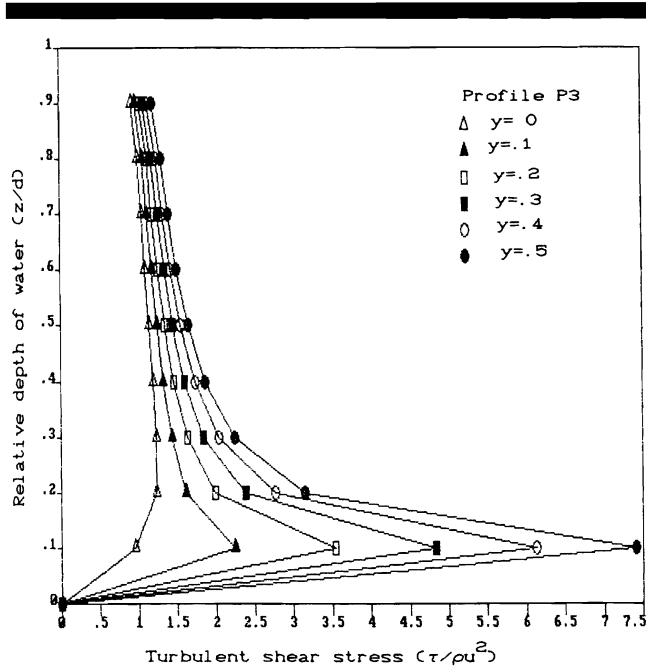


Figure 15. Variation of the profile of  $(\tau/\rho u^2)$  in the y-direction.

16 shows good agreement between the analytical results obtained for profile P7 and the flume data of LYN (1988) for equilibrium bed and for starved bed. Figure 17 shows a plot of  $(\tau/\tau_{\max})$  versus  $(z/d)$  for the averaged profile of P6 and P7, which is obtained by taking for each value of  $(z/d)$  the average

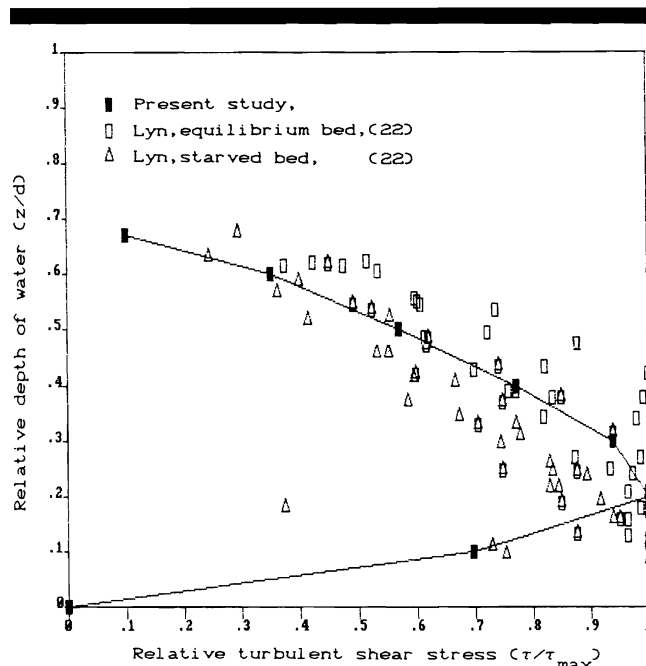


Figure 16. Verification of the profile of the relative turbulent shear stress using the experimental data of Lyn (1988).

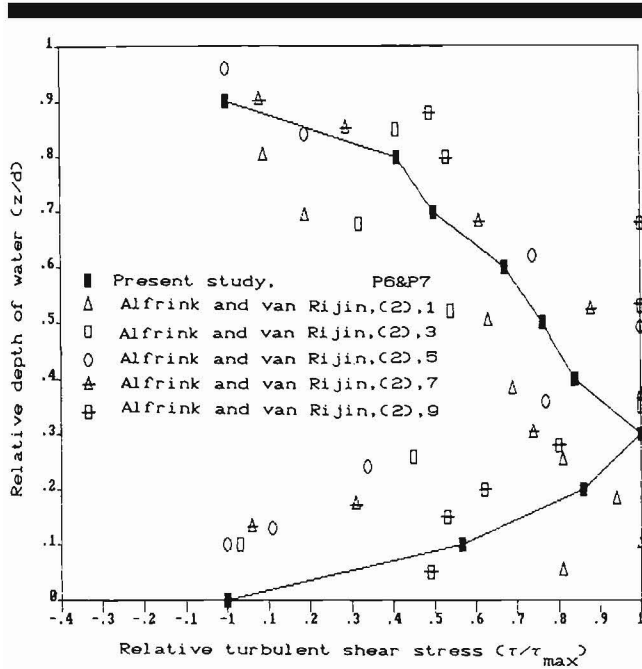


Figure 17. Verification of the profile of the relative turbulent shear stress using the experimental data of Alfrink and van Rijn (1983).

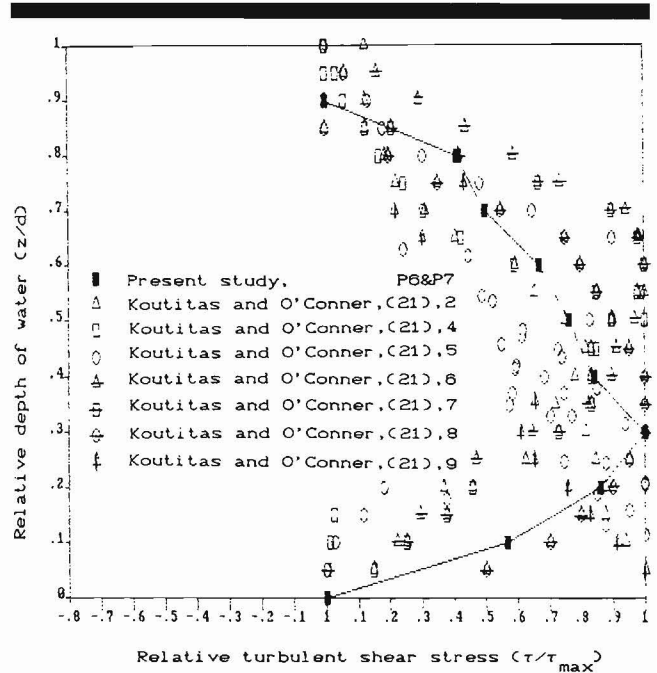


Figure 18. Verification of the profile of the relative turbulent shear stress using the experimental data of Koutitas and O'Conner (1981).

of the two values of  $(\tau/\tau_{max})$  for profiles P6 and P7, and for the flume data of ALFRINK and VAN RIJIN (1983) for the sets of experiments number 1, 3, 5, 7, and 9. The figure shows fair agreement between the analytical results and the experimental ones. The agreement does not appear to be correlated with the type of velocity profile measured by ALFRINK and VAN RIJIN (1983), *e.g.* for the turbulent shear stress data from the sets of experiments number 1 and 9, the velocity profile is nearly logarithmic while for 3 and 5 there is return flow near the bottom, yet the values of  $(\tau/\tau_{max})$  for both types of velocity profiles are equally scattered about the shear stress profile of the present study which is for a logarithmic velocity profile. Figure 18, which is a plot of  $(\tau/\tau_{max})$  versus  $(z/d)$  for the averaged profile of P6 and P7 and for the flume data of KOUTITAS and O'CONNOR (1981) for the sets of experiments number 2, 4, 5, 6, 7, 8, and 9, shows fair agreement between the analytical and the experimental results. Here also the agreement does not appear to be correlated with the type of velocity profile measured by KOUTITAS and O'CONNOR (1981). The only fair agreement between the analytical findings and the experimental results of ALFRINK and VAN RIJIN (1983) and KOUTITAS and O'CONNOR (1981) is likely to be due to the difference in the hydraulic conditions of the present study and the studies of ALFRINK and VAN RIJIN (1983) and KOUTITAS and O'CONNOR (1981) as stated earlier in this section. To summarize the experimental verification, the experimental results presented in Figures 16–18 are combined in Figure 19 which shows that the relative turbulent shear stress profiles obtained from the present study and from the experiments of ALFRINK and VAN RIJIN (1983), KOUTITAS and O'CONNOR (1981), and LYN (1988) have the same trend

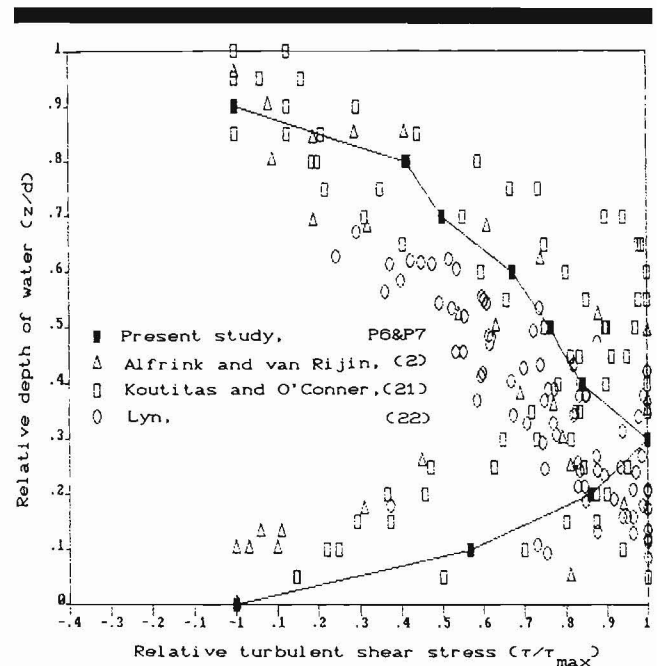


Figure 19. Verification of the profile of the relative turbulent shear stress using the experimental data of Alfrink and van Rijn (1983), Koutitas and O'Conner (1981), and Lyn (1988).

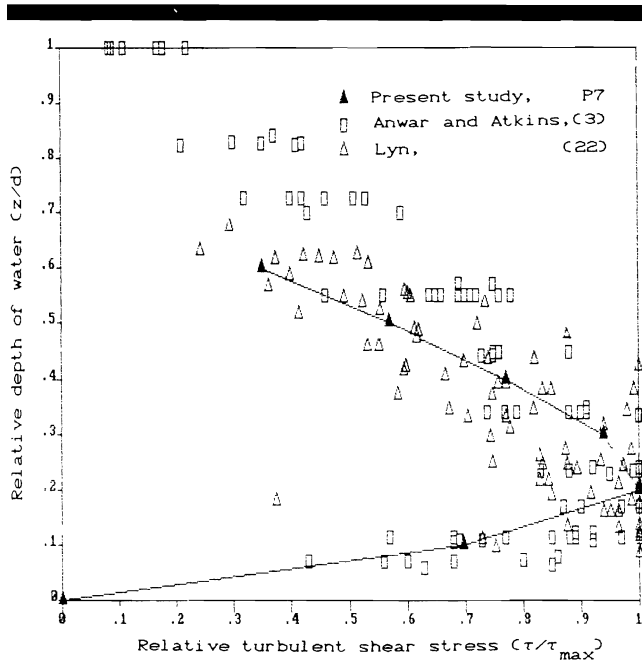


Figure 20. Comparison between the profile of the relative turbulent shear stress for clear water and for sediment laden flows using the experimental data of Anwar and Atkins (1980), and Lyn (1988).

in that the shear stress increases from zero at the bottom, to a maximum value at some distance away from the bottom then decreases towards the water surface.

It is worth noting that the presence of sediment causes the shear stress profile to deviate from that for clear water flow in the upper region of the flow where  $(z/d)$  is larger than about 0.5 as shown in Figure 20. The figure shows a plot of  $(\tau/\tau_{\max})$  versus  $(z/d)$  for profile P7 of the present study and for the flume data of LYN (1988) for sediment laden flow and of ANWAR and ATKINS (1980) for clear water tidal flow. It can be seen from Figure 20 that for  $(z/d)$  larger than about 0.5, the data for clear water flow gives larger values of  $(\tau/\tau_{\max})$  for the same value of  $(z/d)$  than the data for sediment laden flow indicating that the presence of sediment causes a faster dampening of the profile of the relative turbulent shear stress towards the water surface. Similar results were obtained by COLMAN (1969) who interpreted his flume data on velocity profiles with suspended sediment, to mean that the presence of suspended sediment reduces turbulence effects in the outer part of the flow.

### The Longitudinal Velocity of the Flow

The results for the longitudinal velocity of the flow are given in Figures 21–23. Figure 21, a plot of the relative velocity  $(u/U)$  versus the relative depth of water  $(z/d)$  for the seven concentration profiles P1–P7 and for the logarithmic velocity profile, shows that the velocity profiles are nearly logarithmic. The figure is plotted using ENG1 of Enertronics Research Inc. 1983 which, due to the large change in the slope of the velocity profile in the vicinity of  $(z/d) = 0.1$ , cannot draw a

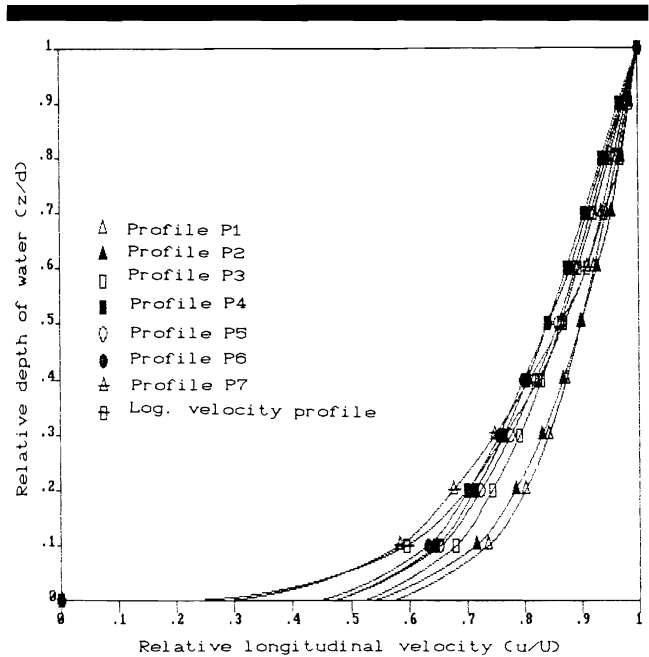


Figure 21. Variation of the relative longitudinal velocity with the relative depth of water.

smooth curve starting from the origin to the value of  $(u/U)$  at  $(z/d) = 0.1$  without having the curve go slightly below the  $x$ -axis [ $(z/d) < 0$ ], this resulted in curves which intercepted the  $(u/U)$  axis at  $(z/d) = 0$ . The effect of the concentration on the velocity profiles is shown in Figures 22 and 23. Figures 22a and 22b show a plot of  $(u/U)$  versus  $(z/d)$  for profiles P1 and P7 respectively for bottom concentrations  $c_0 = 1, 1.2214, 1.4918, 1.8221, 2.2255, \text{ and } 2.7183$ . It can be seen from Figure 22a that the variation in bottom concentration does not have an effect on the profile of the relative velocity; similar results are obtained for profiles P2–P6. For profile P7 however, Figure 22b shows that an increase in the bottom concentration results in a decrease in the relative velocity  $(u/U)$ , *i.e.* a steepening of the relative velocity profile. Figure 23 shows a plot of  $[u/U(c_0 = 1)]$  versus  $(z/d)$  for profile P2. Herein  $U(c_0 = 1)$  is the water surface velocity at the beginning of the estuary and is equal to unity. The figure shows that an increase in bottom concentration  $c_0$  results in an increase in the longitudinal velocity  $u$ .

The experimental data of ASCE (1963), BARTON and LIN (1955), EINSTEIN and CHIEN (1955), LYN (1988), and VANONI and BROOKS (1957) is used for the verification of the results obtained for the longitudinal velocity of the flow as shown in Figures 24–26. Figure 24 shows a plot of the relative longitudinal velocity  $(u/U)$  versus the relative depth of water  $(z/d)$  for the seven concentration profiles P1–P7 and for the experimental data of BARTON and LIN (1955), EINSTEIN and CHIEN (1955), LYN (1988), and VANONI and BROOKS (1957). It can be seen from the figure that good agreement is obtained between the analytical and the experimental results. Figure 25 shows a plot of  $(u/U)$  versus  $(z/d)$  for profile P7, for bottom concentration  $c_0$ , varying from 1.0 to 2.7183, and for

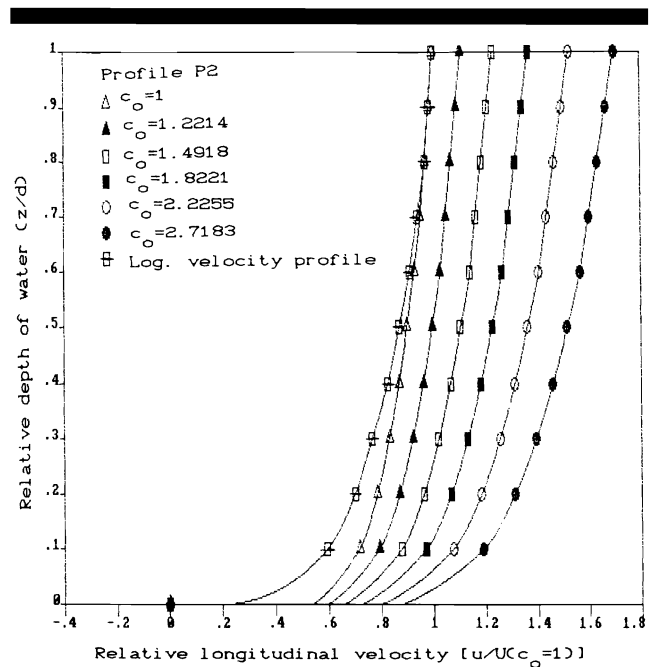
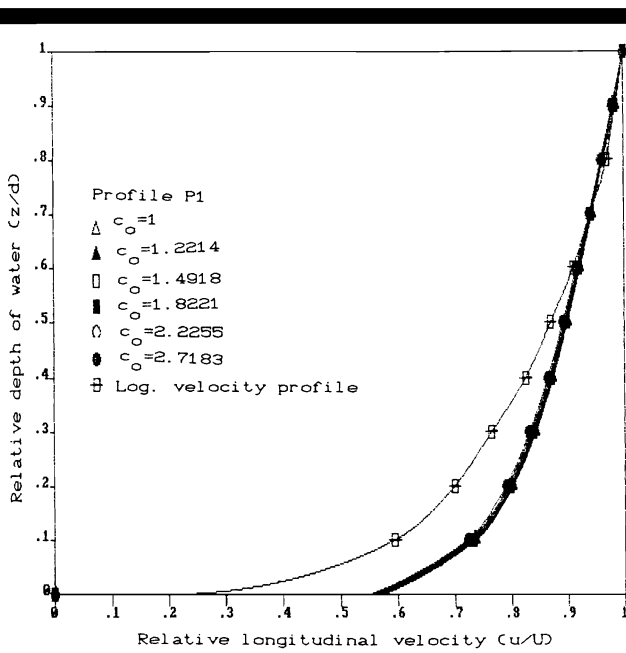


Figure 23. Effect of the concentration of suspended sediment on the profile of the longitudinal velocity.

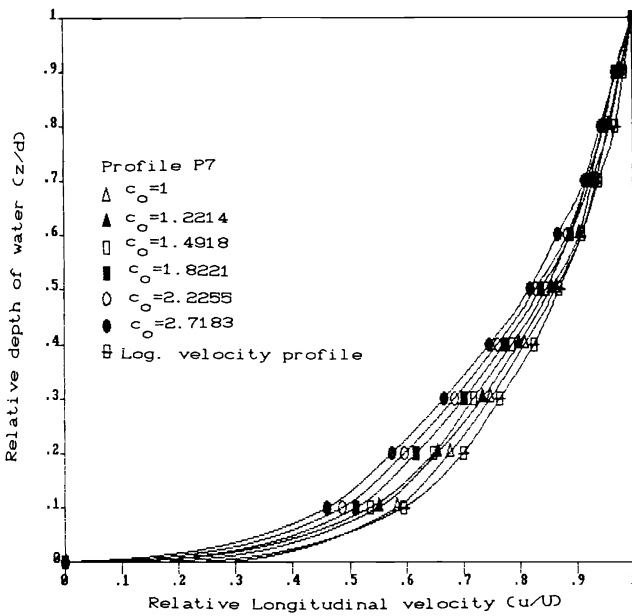


Figure 22 a and b. Effect of the concentration of suspended sediment on the profile of the relative longitudinal velocity.

the experimental data of ASCE (1963) for clear water and for a concentration of 15.8 (g/l). The figure shows that an increase in bottom concentration would result in a steepening of the velocity profile particularly near the bottom, e.g. for a given value of  $(z/d)$  the value of  $(u/U)$  for  $(c_o = 1)$  is larger than for  $(c_o = 1.2214)$ . The experimental data of ASCE (1963) exhibits the same trend, i.e. the profile for a concentration of 15.8 (g/l) is steeper than the profile for clear water. The agreement between the analytical and the experimental re-

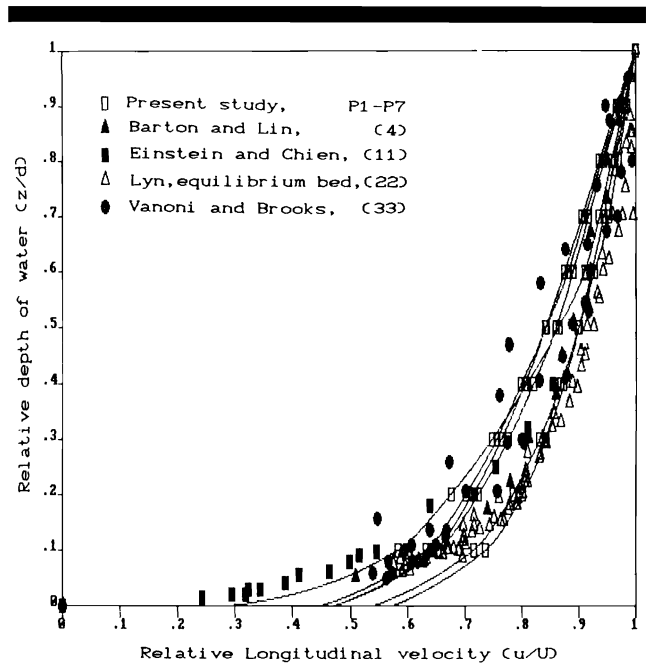


Figure 24. Verification of the profile of the relative longitudinal velocity using the experimental data of Barton and Lin (1955), Einstein and Chien (1955), Lyn (1988), and Vanoni and Brooks (1957).

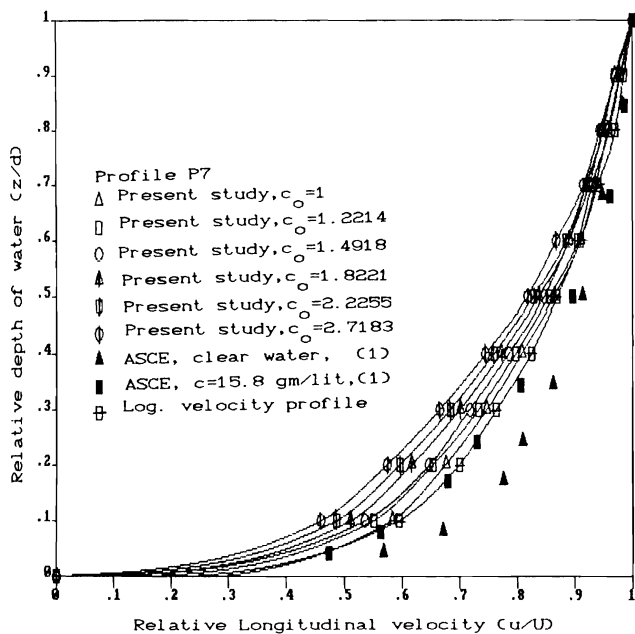


Figure 25. Verification of the profile of the relative longitudinal velocity using the experimental data of ASCE (1963).

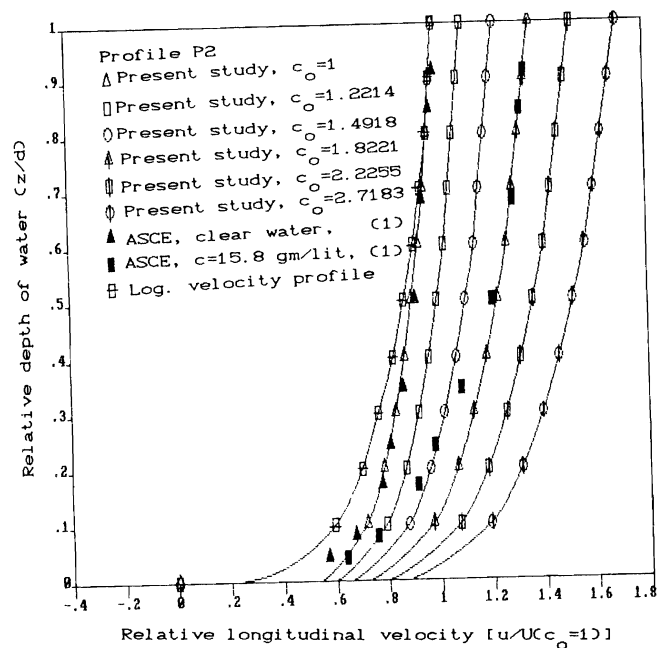


Figure 26. Verification of the profile of the longitudinal velocity using the experimental data of ASCE (1963).

sults is only fair perhaps because the experimental data reported in ASCE (1963) gives a considerably flatter velocity profile than the logarithmic velocity profile, *e.g.* the velocity profile for  $c_o = 15.8$  (g/l) coincides with the logarithmic velocity profile for  $(z/d)$  values between 0 and 0.3 then becomes flatter, and the profile for clear water is even more flat instead of coinciding with the logarithmic velocity profile. Figure 26 shows a plot of  $[u/U(c_o = 1)]$  versus  $(z/d)$  for profile P2, for bottom concentration  $c_o$ , varying from 1.0 to 2.7183 and for the experimental data given in ASCE (1963). It can be seen from the figure that the experimental data confirms the analytical findings that an increase in the concentration results in an increase in the relative longitudinal velocity. COLMAN (1969) reported that transported sediment increases the velocity at all elevations with the increase being progressively greater at large distances from the bed. LYN (1988) also reported that the presence of sediment causes the velocity profile to deviate from the clear water velocity profile with the deviation increasing with increasing suspended load but the effect of the presence of sediment on the velocity profile is confined to a layer adjacent to the bed.

### Effect of Concentration on von Karman's ( $\kappa$ )

It would be interesting to examine the analytical solution presented in the present study in the light of the recent work of COLMAN (1981) on the effect of sediment concentration on the velocity profile. For this reason the logarithmic velocity profile, rather than the power law velocity profile presented in ROUSE (1959), is used in the construction of the solution of the zeroth approximation. Early work on the effect of the concentration of suspended sediment on von Karman's  $\kappa$

[EINSTEIN and CHIEN (1955), ELATA and IPPEN (1961), and VANONI (1946)], shows that  $\kappa$  decreases with an increase in the concentration of suspended sediment. This is stated in books on sediment transport such as that by GRAF (1971). COLMAN (1981) re-analyzed early data together with new data of his own according to his method (COLMAN, 1981), and showed that  $\kappa$  is essentially constant over a wide range of flows varying from flows with no sediment suspension to flows with near capacity load of suspended sediment. According to COLMAN (1981) the reason for the contradiction between the results obtained by his method and by the traditional method, (VANONI, 1946), is that the traditional method does not take into consideration the existence of the wake region which was not known to researchers on sediment transport at the time the traditional method was developed.

The results obtained, from the present study, for von Karman's  $\kappa$  are given in Figure 27 which shows a plot of the bottom concentration  $c_o$  versus  $\kappa$  computed according to the traditional method of VANONI (1946) and to the more recent method of COLMAN (1981). The concentration near the bottom  $c_o$  is presented as a percentage of concentration by volume and plotted on logarithmic scale. In the figure the results are fitted by a linear regression and show that Colman's method gives higher values for  $\kappa$  than the traditional method of VANONI (1946). The figure also shows a significant decrease in  $\kappa$ , with an increase in the concentration of suspended sediment, when the results are analyzed by the traditional method; this would be more clear when the percentage of concentration by volume is plotted on arithmetic scale, although such a plot is not given here in order to save journal space.

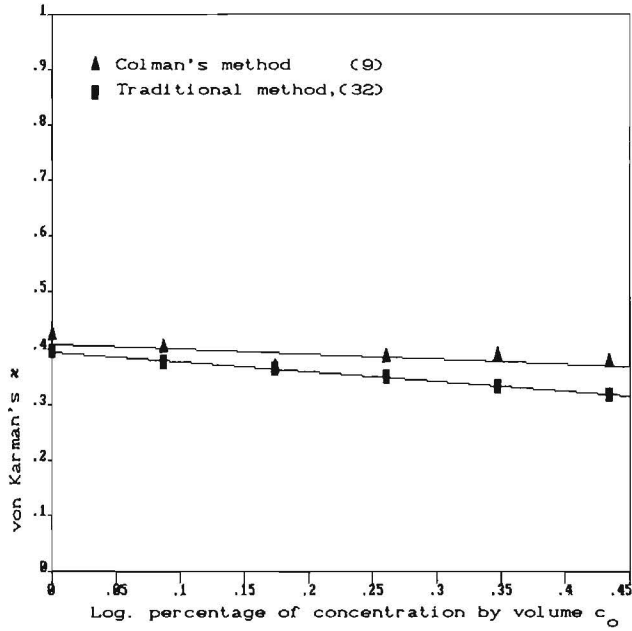


Figure 27. Effect of the concentration of suspended sediment on von Karman's  $\kappa$  computed by the recent method of Colman (1981) and by the traditional method of Vanoni (1946).

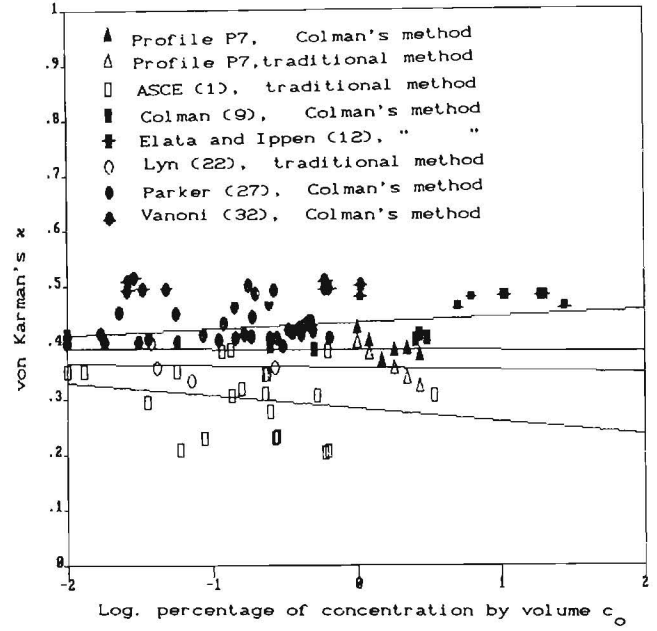


Figure 28. Verification of the effect of the concentration of suspended sediment on von Karman's  $\kappa$  using the experimental data of ASCE (1963), Colman (1981), Elata and Ippen (1961), Lyn (1988), Parker and Colman (1986), and Vanoni (1946) taken from Colman (1981).

The verification of the analytical results with the flume data of ASCE (1963), COLMAN (1981), ELATA and IPPEN (1961), LYN (1988), PARKER and COLMAN (1986), and VANONI (1946) taken from COLMAN (1981); is shown in Figure 28. Some of the data of IPPEN (1961) is not shown in the figure because the data is for a much higher concentration than that used by the other investigators which makes it inconvenient to include in the figure. In the figure both the analytical results and the flume data are fitted by a linear regression. The top line is the regression line for the flume data analyzed by COLMAN'S (1981) method; the second line from the top is for the analytical results analyzed by the same method. The third line is the regression line for the analytical results analyzed by the traditional method and the bottom line is for the flume data analyzed by the same method. Figure 28 shows good qualitative agreement between the analytical and the experimental results in that Colman's method gives higher values for  $\kappa$  than the traditional method and that the traditional method gives a significant decrease in  $\kappa$  with an increase in the concentration of suspended sediment.

**CONCLUSIONS**

The equations of conservation of volume, mass, and momentum, and the equation of kinetic energy of turbulence, are formulated for the three dimensional flow of a mixture of water and sediment. The equations are closed and expressed in dimensionless form to represent conditions in well mixed estuaries for ebb flow departing from slack. This results in four partial differential equations (eqs. 8, 27, 29, and 30) for the conservation of volume, of mass, and of momentum in the

y and z-directions, and two integro differential equations (eqs. 28 and 31) for the conservation of momentum in the x-direction and for the kinetic energy of turbulence.

Nine  $\pi$ -terms appear namely; the aspect ratios (R/L) and (R/W); the density gradient ( $\Delta\rho/\rho$ ); a form of Ekman number  $E = (\epsilon_{max}/f L^2)$ ; Reynolds number  $R = (U R \rho_w/\mu_w)$ ; a form of Richardson number  $R_* = (U^2/(\Delta\rho/\rho) g R)$ ; Rossby number  $R_{**} = (U/f L)$ ; and two forms of an eddy Reynolds number namely,  $R^* = (\rho U^2/\tau_{max})$  and  $R^{**} = (U R/\epsilon_{max})$ . The numerical values of the nine  $\pi$ -terms are as follows: (R/L) =  $4.458 \times 10^{-5}$ , (R/W) =  $4.38 \times 10^3$ , ( $\Delta\rho/\rho$ ) = 0.1416,  $E = 1.05 \times 10^{-7}$ ,  $R = 1.6568 \times 10^9$ ,  $R_* = 1.0414 \times 10^{-4}$ ,  $R_{**} = 2.121 \times 10^{-3}$ ,  $R^* = 1.445$ , and  $R^{**} = 0.8968$ . The magnitude of each term in eqs. 27-31 is evaluated and the  $\pi$ -terms (R/L), (R/W), E,  $R^{-1}$ ,  $R_*$ , and  $R_{**}$  are used as perturbation parameters.

The zeroth approximation is obtained by setting the perturbation parameters equal to zero; this results in five partial differential equations (eqs. 38, 39, 41, 42, and 43) for the conservation of volume, of mass, and of momentum in the y and z-directions, and for the kinetic energy of turbulence, and an integro differential equation (eq. 40) for the conservation of momentum in the x-direction. The solution of the zeroth approximation is presented as a Fourier series of the eigenfunctions ( $\phi_n$ ) =  $(2)^{1/2} \sin(\lambda_n^{1/2} z)$ , of the Sturm-Liouville problem  $\zeta'' + \lambda_n \zeta = 0$ ,  $\zeta(0) = 0$ ,  $\zeta(1) = 0$ ; where the eigenvalues  $\lambda_n = (n\pi)^2$ ,  $n = 1, 2, \dots$

The solution of the zeroth approximation for the concentration of suspended sediment  $c(x, z)$  shows that the concentration increases along the estuary in the downstream direction, as shown in Figure 9; this is in agreement with previous re-

search work on sedimentation. The results obtained for the coefficient of exchange of mass  $\epsilon$  show that  $\epsilon$  increases from zero at the bottom of the estuary to a maximum value at a relative depth ( $z/d$ ) of about 0.1 then decreases to a nearly constant value towards the water surface as shown in Figure 10. This is in agreement with the distribution of  $\epsilon$  reported by ICHIYE (1966) for the nepheloid layer on the Atlantic slope.

The results obtained for the turbulent shear stress  $\tau$  show that: (1)  $(\tau/\rho u^2)$  increases from zero at the bottom of the estuary to a maximum value at ( $z/d$ ) of about 0.2 then decreases towards the water surface as shown in Figures 12–15. (2) For the same bottom concentration  $c_o$ ,  $(\tau/\rho u^2)$  decreases with the increase in the uniformity of the concentration distribution, as shown in Figure 12; e.g.  $(\tau/\rho u^2)$  for profile P1, where the concentration distribution decays rapidly towards the water surface is larger than  $(\tau/\rho u^2)$  for profile P7 where the concentration distribution is more uniform. (3) For the same concentration profile,  $(\tau/\rho u^2)$  is nearly invariant for the different bottom concentrations  $c_o$ , as shown in Figure 13. Also  $(\tau/\rho u^2)/(\tau/\rho u^2)_{\max}$  is invariant with the bottom concentration as shown in Figure 14. (4)  $(\tau/\rho u^2)$  increases away from the center line of the estuary towards the sides as shown in Figure 15.

The flume data of ALFRINK and VAN RIJIN (1983), ANWAR and ATKINS (1980), KOUTITAS and O'CONNOR (1981), and LYN (1988) is used for the verification of the turbulent shear stress results obtained from the present study as shown in Figures 16–20 which give a plot of  $(\tau/\tau_{\max})$  versus ( $z/d$ ). Of the above flume data that of LYN (1988) is the only data which corresponds to conditions similar to the present study in that the data is for turbulent open channel flow over a flat sand bed in equilibrium with a suspension of sand. The data of ALFRINK and VAN RIJIN (1983) is for a steep-sided trench perpendicular to the mean flow direction, the data of KOUTITAS and O'CONNOR (1981) is for a steep-sided channel dredged at right angles to the main direction of the flow and sediment transport, and the data of ANWAR and ATKINS (1980) is for clear water tidal flow. Figure 16 shows good agreement between the analytical findings of the present study and the flume data of LYN (1988). Figures 17 and 18 respectively, show only fair agreement between the analytical findings and the experimental results of ALFRINK and VAN RIJIN (1983) and of KOUTITAS and O'CONNOR (1981) in view of the difference in the hydraulic conditions for which the present study is formulated and the hydraulic conditions under which the experimental data was collected. Figure 19 shows a comparison between the turbulent shear stress profiles obtained from the present study and from the experiments of ALFRINK and VAN RIJIN (1983), KOUTITAS and O'CONNOR (1981), and LYN (1988) which are shown in Figures 16–18. It can be seen from Figure 19 that the profiles obtained from the present study and from the flume data of ALFRINK and VAN RIJIN (1983), KOUTITAS and O'CONNOR (1981), and LYN (1988) exhibit the same trend in that the turbulent shear stress increases from zero at the bottom to a maximum value at some distance away from the bottom then decreases towards the water surface. Figure 20 shows that the presence of sediment causes the shear stress profile to deviate from that for clear water flow in the upper region of the flow where ( $z/d$ ) is larger than about 0.5 indicating a fast-

er dampening of the profile of the relative turbulent shear stress towards the water surface for sediment laden flow (LYN, 1988) than for clear water flow (ANWAR and ATKINS, 1980).

The results obtained from the present study for the longitudinal velocity of the flow are given in Figures 21–23 and indicate that: (1) The velocity profiles are nearly logarithmic as shown in Figure 21. This is verified in Figure 24 which shows good agreement between the velocity profiles obtained from the present study and the experimental data of BARTON and LIN (1955), EINSTEIN and CHIEN (1955), LYN (1988), and VANONI and BROOKS (1957). (2) The profile of the relative velocity appears to be invariant with bottom concentration; this is particularly so for profiles P1–P6 as shown in Figure 22a for profile P1. For profile P7, an increase in bottom concentration results in a steepening of the profile of the relative velocity as shown in Figure 22b. This is verified in Figure 25 which shows fair agreement between the velocity profiles obtained from the present study, for bottom concentrations varying from 1 to 2.7183, and the experimental data of ASCE (1963). (3) An increase in bottom concentration results in an increase in the longitudinal velocity as shown in Figure 23 and verified in Figure 26 which shows fair agreement between the results obtained from the present study and the data of ASCE (1963). This is in agreement with COLMAN (1969) who reported that transported sediment increases the velocity at all elevations. LYN (1988) also reported that the increase in the concentration causes the velocity profile to deviate more from the clear water velocity profile although the deviation is confined to a layer adjacent to the bed.

Analysis of profile P7 for the effect of the concentration of suspended sediment on von Karman's  $\kappa$  shows that: (1) Colman's method (COLMAN, 1981) gives higher values for  $\kappa$  than the traditional method (VANONI, 1946) as shown in Figure 27. This is in agreement with the experimental data of ASCE (1963), COLMAN (1981), ELATA and IPPEN (1961), LYN (1988), PARKER and COLMAN (1986), and VANONI (1946) as shown in Figure 28. (2) There is a significant decrease in  $\kappa$  with an increase in the concentration of suspended sediment, when the velocity profiles are analyzed by the traditional method as shown in Figure 27 (this would be more clear when the percentage of concentration by volume is plotted on arithmetic scale rather than on logarithmic scale; such a plot is not shown here in order to save journal space). This is in agreement with the experimental data of ASCE (1963), COLMAN (1981), ELATA and IPPEN (1961), LYN (1988), PARKER and COLMAN (1986), and VANONI (1946) as shown in Figure 28.

## ACKNOWLEDGEMENTS

The study was initiated while the writer was a visiting scholar with the Department of Civil Engineering, University of California at Berkeley, and was continued with the Department of Mathematics. The writer would like to express his sincere thanks to Professor J. A. Harder of the Department of Civil Engineering and to Professors P. L. Chambre and H. O. Cordes of the Department of Mathematics of the University of California at Berkeley.

## LITERATURE CITED

- AMERICAN SOCIETY OF CIVIL ENGINEERS TASK COMMITTEE ON PREPARATION OF SEDIMENTATION MANUAL, 1963. Sediment transportation mechanics: suspension of sediment. *Journal of the Hydraulics Division, ASCE*, 5, 45-76.
- ALFRINK, B.J. and VAN RIJIN, L.C., 1983. Two-equations turbulence model for flow in trenches. *Journal of Professional Issues in Engineering (ASCE)*, 109(3), 941-958.
- ANWAR, H.O. and ATKINS, R., 1980. Turbulence measurements in simulated tidal flow. *Journal of the Hydraulics Division (ASCE)*, 106(HY8), 1273-1289.
- BARTON, J.R. and LIN, P.N., 1955. A study of the sediment transport in alluvial channels. *Report No. 55 JR82, Colorado A&M College, Civil Engineering Department, Fort Collins, Colorado.*
- BRADSHAW, P.; FERRIS, D.H., and ATWELL, N.P., 1967. Calculation of boundary layer development using the turbulent energy equation. *Journal of Fluid Mechanics*, 28, 593-616.
- CHAMBRE, P.L., 1977. Integral equations, (unpublished lecture notes). *Department of Mathematics, University of California, Berkeley, California.*
- CHIU, C.L. and HSIUNG, D.E., 1981. Secondary flow, shear stress and sediment transport. *Journal of the Hydraulics Division (ASCE)*, 107(HY7), 879-898.
- COLMAN, N.L., 1969. A new examination of sediment suspension in open channels. *Journal of Hydraulic Research*, 7(1), 67-82.
- COLMAN, N.L., 1981. Velocity profiles with suspended sediment. *Journal of Hydraulic Research*, 19(3), 211-229.
- EAGLESON, P.S., (ed.), 1966. *Estuary and Coastline Hydrodynamics*. New York: McGraw-Hill.
- EINSTEIN, H.A. and CHIEN, N., 1955. Effect of heavy sediment concentration near the bed on velocity and sediment distribution. *MRD Series no. 8*, University of California Institute of Engineering Research and U.S. Army Corps of Engineers, Missouri River Division, Omaha, Nebraska.
- ELATA, C. and IPPEN, A.T., 1961. The dynamics of open channel flow with neutrally buoyant particles. *Hydrology Laboratory Report No. 45*, Massachusetts Institute of Technology, 69p.
- GRAF, W.H., 1971. *Hydraulics of Sediment Transport*. New York: McGraw-Hill.
- ICHIYE, T., 1966. Some hydrodynamic problems for a nepheloid zone. *Review Pure and Applied Geophysics*, 63, 179-195.
- KAMEL, A.M., 1972. Evaluation and interpretation of the physical data for the Delaware Bay and estuary, (unpublished report). College of Marine Studies, University of Delaware, Newark, Delaware.
- KAMEL, A.M., 1976. The mechanics of estuarine shoaling, (unpublished report). Division of Hydraulics and Coastal Engineering, University of California, Berkeley, California.
- KAMEL, A.M., 1978. The mechanics of sediment suspension, (unpublished report). Division of Hydraulics and Coastal Engineering, University of California, Berkeley, California.
- KAMEL, A.M., 1987. Mechanics of sediment suspension in well mixed estuaries, (unpublished report). Engineering Science Research Center, University of Gar Younis, Benghazi.
- KAMKE, E., 1971. *Differentialgleichungen Lösungsmethoden und Lösungen*, Band 1, New York: Chelsea.
- KARIM, M.F. and KENNEDY, J.F., 1987. Velocity and sediment concentration profiles in river flows. *Journal of Hydraulic Engineering (ASCE)*, 113(1), 159-177.
- KOUTITAS, C. and O'CONNOR, B., 1981. Turbulence model for flow over dredged channels. *Journal of the Hydraulics Division (ASCE)*, 107(HY8), 989-1002.
- LYN, D.A., 1988. A similarity approach to turbulent sediment-laden flows in open channels. *Journal of Fluid Mechanics*, 193, 1-26.
- MILLMAN, M.H. and KELLER, J.L., 1969. Perturbation theory of non-linear boundary value problems. *Journal of Mathematical Physics*, 10, 342-361.
- MONIN, A.S. and YAGLOM, A.M., 1971. *Statistical Fluid Mechanics*, vol. 1. Cambridge, Massachusetts: M.I.T. Press.
- MYINT-U.T., 1987. *Partial Differential Equations for Scientists and Engineers*. New York: Elsevier.
- NAYFEH, A.H., 1985. *Problems in Perturbation*. New York: Wiley.
- PARKER, G. and COLMAN, N.L., 1986. Simple model of sediment-laden flows in open channels. *Journal of Hydraulic Engineering (ASCE)*, 112(5), 356-375.
- PEDLOSKEY, J., 1987. *Geophysical Fluid Dynamics*. New York: Springer-Verlag.
- ROUSE, H., (ed.), 1959. *Advanced Mechanics of Fluids*. New York: Wiley.
- SOO, S.L., 1967. *Fluid Dynamics of Multi-Phase Systems*. Waltham, Massachusetts: Blaisdell.
- TENNEKES, H. and LUMELY, J.L., 1972. *A First Course in Turbulence*. Cambridge, Massachusetts: M.I.T. Press.
- VANONI, V.A., 1946. Transportation of suspended sediment by water. *Transactions ASCE*, III, 67-133.
- VANONI, V.A. and BROOKS, N.H., 1957. Laboratory study of the roughness and suspended load of alluvial streams. Report no. E-68, California Institute of Technology, Pasadena, California.
- VAN DYKE, M., 1964. *Perturbation methods in fluid mechanics*. New York: Academic.
- VAN RIJIN, L.C., 1984. Sediment transport, part 2: suspended load transport. *Journal of Hydraulic Engineering, (ASCE)*, 110(11), 1613-1641.
- VASELIEV, O.P., 1969. Problems of two phase flow theory. *Proceedings of 13th Congress of IAHR (Kyoto, Japan)*, pp. 40-74.

## APPENDIX I. NOTATION

The following symbols are used in this paper.

- a = numerical constant.
- A = maximum tidal amplitude.
- c = concentration of suspended sediment by volume.
- $c_a$  = concentration of suspended sediment by volume at a distance (a) from bottom of channel.
- $c_o$  = concentration of suspended sediment by volume at bottom of estuary.
- d = average water depth in estuary.
- E = Ekman number.
- f = Coriolis parameter =  $2\Omega \sin \theta$ , taken as  $10^{-4}$  (sec<sup>-1</sup>).
- g = acceleration due to gravity.
- G = closure function for diffusion.
- i, j, k = indices.
- ℓ = mixing length.
- L = length of estuary.
- ℓ = dissipation length parameter.
- n = Manning's coefficient of roughness.
- p = pressure.
- R = hydraulic radius of estuary.
- R = Reynolds number.
- $R_*$  = Richardson number.
- $R_{**}$  = Rossby number.
- $R^*, R_{**}$  = eddy Reynolds numbers.
- S = slope of water surface of estuary.
- t = time.
- u, v, w = respectively, longitudinal, transverse, and vertical velocities of flow.
- U = longitudinal velocity at free surface.
- U = depth averaged longitudinal velocity for ebb flow departing from slack.
- $U_1$  = outer velocity = 1.
- $u_*$  = shear velocity.
- $u_{*o}$  = shear velocity at bottom of estuary.

$W$	= average width of estuary.				
$\dot{w}$	= settling velocity of sediment particles.				
$x, y, z$	= respectively, longitudinal, transverse, and vertical coordinates.	$\theta$		= angle between water surface in estuary and horizontal.	
$X, Z$	= dependent variables, functions of $x$ and $z$ , respectively.	$\Omega$		= component of the earth's rotation vector.	
$\alpha$	= numerical constant.	$\Delta, \psi, \sigma, \omega, \zeta$		= functions of ( $z$ ).	
$\alpha_n$	= coefficient of Fourier series.	$\phi_n$		= eigenfunctions.	
$\beta$	= separation constant.	$\tau$		= turbulent shear stress.	
$\gamma$	= a number dependent on the separation constant $\beta$ .	$\tau_o$		= turbulent shear stress at bottom of estuary.	
$\lambda_n$	= eigenvalues.	$v, \varphi, \Phi, \xi, \eta$		= dependent variables, functions of $z$ .	
$\delta$	= thickness of boundary layer = 1.	Superscripts:			
$\epsilon$	= coefficient of exchange of mass.	'		= fluctuation from the mean.	
$\epsilon$	= dissipation term.	-		= mean value.	
$\kappa$	= von Karman's constant.	Subscripts:			
$\mu$	= dynamic viscosity.	m		= mixture of water and sediment.	
$\nu$	= kinematic viscosity.	max		= maximum value.	
$\rho$	= density.	o		= zeroth approximation.	
$\Delta\rho$	= maximum difference between the densities of the water-sediment mixture and that of water = $(\rho_{\max} - \rho_w)$ .	s		= sediment.	
		w		= water.	